Two novel members of the LhrC family of small RNAs in Listeria monocytogenes with overlapping regulatory functions but distinctive expression profiles

Mollerup, Maria Storm; Ross, Joseph; Helfer, AC; Meistrup, Kristine; Romby, Pascale; Kallipolitis, Birgitte H.

Published in:
R N A Biology

DOI:
10.1080/15476286.2016.1208332

Publication date:
2016

Document version
Final published version

RNA Biology

ISSN: 1547-6286 (Print) 1555-8584 (Online) Journal homepage: http://www.tandfonline.com/loi/krnb20

Two novel members of the LhrC family of small RNAs in Listeria monocytogenes with overlapping regulatory functions but distinctive expression profiles

Maria Storm Mollerup, Joseph Andrew Ross, Anne-Catherine Helfer, Kristine Meistrup, Pascale Romby & Birgitte Haahr Kallipolitis

To cite this article: Maria Storm Mollerup, Joseph Andrew Ross, Anne-Catherine Helfer, Kristine Meistrup, Pascale Romby & Birgitte Haahr Kallipolitis (2016) Two novel members of the LhrC family of small RNAs in Listeria monocytogenes with overlapping regulatory functions but distinctive expression profiles, RNA Biology, 13:9, 895-915, DOI: 10.1080/15476286.2016.1208332

To link to this article: http://dx.doi.org/10.1080/15476286.2016.1208332

RNA BIOLOGY
2016, VOL. 13, NO. 9, 895–915
http://dx.doi.org/10.1080/15476286.2016.1208332

Taylor & Francis
Taylor & Francis Group

RESEARCH PAPER

Two novel members of the LhrC family of small RNAs in *Listeria monocytogenes* with overlapping regulatory functions but distinctive expression profiles

Maria Storm Mollerup[a], Joseph Andrew Ross[a], Anne-Catherine Helfer[b], Kristine Meistrup[a], Pascale Romby[b], and Birgitte Haahr Kallipolitis[a]

[a]Department of Biochemistry and Molecular Biology, University of Southern Denmark, Odense, Denmark; [b]Architecture et Réactivité de l'ARN, Université de Strasbourg, CNRS, IBMC, Strasbourg, France

ABSTRACT

Multicopy small RNAs (sRNAs) have gained recognition as an important feature of bacterial gene regulation. In the human pathogen *Listeria monocytogenes*, 5 homologous sRNAs, called LhrC1-5, control gene expression by base pairing to target mRNAs though 3 conserved UCCC motifs common to all 5 LhrCs. We show here that the sRNAs Rli22 and Rli33-1 are structurally and functionally related to LhrC1-5, expanding the LhrC family to 7 members, which makes it the largest multicopy sRNA family reported so far. Rli22 and Rli33-1 both contain 2 UCCC motifs important for post-transcriptional repression of 3 LhrC target genes. One such target, *oppA*, encodes a virulence-associated oligo-peptide binding protein. Like LhrC1-5, Rli22 and Rli33-1 employ their UCCC motifs to recognize the Shine-Dalgarno region of *oppA* mRNA and prevent formation of the ribosomal complex, demonstrating that the 7 sRNAs act in a functionally redundant manner. However, differential expression profiles of the sRNAs under infection-relevant conditions suggest that they might also possess non-overlapping functions. Collectively, this makes the LhrC family a unique case for studying the purpose of sRNA multiplicity in the context of bacterial virulence.

ARTICLE HISTORY
Received 13 May 2016
Revised 23 June 2016
Accepted 28 June 2016

KEYWORDS
Antisense; *Listeria monocytogenes*; multiplicity; post-transcriptional regulation; sRNAs

Introduction

Gene regulation exerted by small non-coding RNAs (sRNAs) is a key event in all bacterial species. In multiple cases, sRNAs have been shown to be involved in stress tolerance and virulence control, making sRNAs important regulators of bacterial pathogenesis.[1-5] Typically, sRNAs modulate gene expression at the post-transcriptional level by base-pairing to target mRNAs.[2] The most abundant class of base-pairing sRNAs, referred to as *trans*-acting sRNAs, exert their regulatory effect on distantly located target genes. Consequently, base-pairing complementarity is only partial, permitting the recognition of multiple target mRNAs. The canonical mechanism for sRNA-mediated control involves binding of the sRNA to the Shine-Dalgarno (SD) region of a target mRNA, leading to inhibition of ribosome binding and mRNA degradation.[2] The facultative intracellular pathogen *Listeria monocytogenes* serves as a model organism for studies of sRNA-mediated control in Gram-positive species.[6] *L. monocytogenes* is a foodborne pathogen and the causative agent of listeriosis—affecting elderly, immune-compromised people as well as pregnant women—with an estimated fatality rate of 20–30%.[7,8] More than 200 sRNAs have been identified in *L. monocytogenes*,[9-15] several of which have been shown to contribute to listerial pathogenesis.[12,16, 17] However, in the majority of cases, their biological role and mechanism of action remain unexplored.

The continuous discovery of more sRNAs has revealed several examples where 2 or more homologous sRNAs, also known as "sibling sRNAs," are produced in a single bacterium.[18-22] In *L. monocytogenes* LO28, 5 homologous sRNAs constitute the multicopy family LhrC.[15] These 5 sRNAs, named LhrC1-5, are encoded from independent promoters at 2 genomic loci. LhrC1-4 are encoded from the intergenic region of *cysK* and *sul*, whereas LhrC5 is encoded from the intergenic region of *lmo0946* and *lmo0947* (Fig. 1A). Expression of LhrC1-5 is highly induced in response to cell envelope stress via the two-component system LisRK.[23] Furthermore, a strain lacking *lhrC1-5* is impaired in infection of macrophage-like cells, suggesting a putative role in virulence.[24] We recently demonstrated that LhrC1-5 act by an antisense mechanism to down-regulate the expression of specific target mRNAs.[23,24] Although LhrC1-5 were originally identified by Hfq co-immunoprecipitation,[15] neither the stability nor the activity of LhrC1-5 seem to depend on the presence of this RNA chaperone.[15,23,24] So far, 3 direct mRNA targets of LhrC1-5 have been identified. They encode the virulence adhesion LapB;[25] the $CD4^+$ T-cell stimulating antigen TcsA[26] and the oligo-peptide binding protein OppA.[27] These cell envelope associated proteins have all been shown to be important for virulence,[25,27,28] further implicating LhrC1-5 in the regulation of listerial pathogenesis.

CONTACT Birgitte Haahr Kallipolitis bhk@bmb.sdu.dk
Supplemental data for this article can be accessed on the publisher's website.

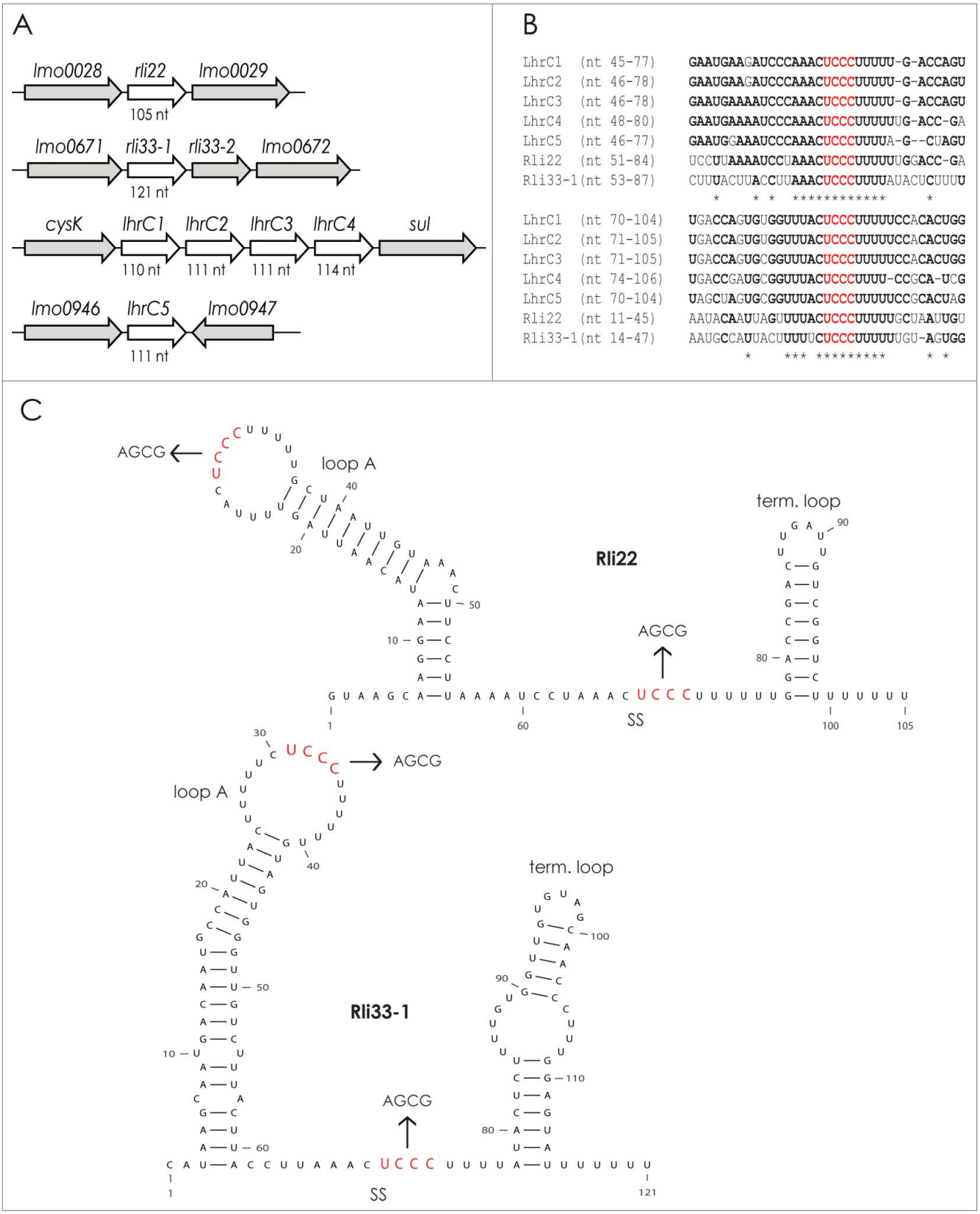

Figure 1. Rli22 and Rli33-1: Two sRNAs related to LhrC1-5. (A) Chromosomal locations and nucleotide lengths of *rli22*, *rli33-1*, *lhrC1-4* and *lhrC5*. Both Rli22 and Rli33-1 are encoded from intergenic regions distant from the chromosomal loci of *lhrC1-4* and *lhrC5*. (B) Sequence alignment of CU-rich regions of Rli22, Rli33-1, and LhrC1-5. Nucleotides shared by a majority of the sRNAs are depicted in bold. Fully conserved nucleotides are indicated by an asterisk. The UCCC motif common to all seven sRNAs is depicted in red. (C) Secondary structures of Rli22 (top) and Rli33-1 (bottom). The CU-rich motifs of Rli22 and Rli33-1 are situated within the loop A region and the single-stranded (ss) region, respectively. The UCCC motifs are depicted in red. For mutational studies of Rli22 and Rli33-1 *in vivo*, the UCCC motifs were substituted by the indicated nucleotides.

Regulatory sRNAs of Gram-positive bacteria often contain CU-rich motifs which are important for target mRNA interaction.[19,29-32] In *L. monocytogenes*, each copy of LhrC contains 3 CU-rich regions, characterized by a conserved UCCC motif.[23,24] While only 2 UCCC motifs in LhrC4 are crucial for the interaction with *oppA* mRNA, all 3 UCCC motifs of LhrC4 target the SD region of *lapB* mRNA. Thus, the multiplicity of CU-rich regions allows simultaneous binding of up to 3 identical (or even different) mRNAs to a single LhrC sRNA.[24] Accordingly, the LhrC family represents a unique case for studies on the purpose of multiplicity and the regulatory interplay between homologous sRNAs in Gram-positive bacteria.

In this study, we demonstrate that the LhrC family of sRNAs is even larger than first anticipated. Two novel members of the LhrC family are revealed: Rli22 and Rli33-1. These sRNAs contain 2 UCCC motifs each and were initially discovered in *L. monocytogenes* by tiling arrays.[14] As demonstrated for LhrC1-5, Rli22 and Rli33-1 use their UCCC motifs to control the expression of the LhrC target genes *tcsA, lapB* and *oppA* at the post-transcriptional level. We show that both UCCC motifs of Rli22 and Rli33-1 are able to bind the SD region of *oppA* mRNA (albeit with different affinities), thereby preventing the formation of the ribosomal complex. These findings clearly demonstrate that Rli22, Rli33-1 and LhrC1-5 are sibling sRNAs with overlapping regulatory functions. However, despite their structural and functional similarities, some differences between the sibling sRNAs could be observed. Like LhrC1-5, Rli22 is induced in response to cell envelope stress in a LisRK-dependent manner, whereas expression of Rli33-1 depends on the general stress sigma factor σ^B. Furthermore, the 7 sRNAs display differential expression profiles under infection-relevant conditions, suggesting that they might also perform non-overlapping regulatory functions in *L. monocytogenes*.

Results

Two novel members of the LhrC family: Rli22 and Rli33-1

In order to search for additional members of the LhrC family, we carried out a BLAST analysis of LhrC1-5 versus annotated sRNAs of *Listeria monocytogenes* EGD-e using the sRNA database sRNAdb.[33] This search revealed 2 sRNAs with homology to all 5 LhrCs: Rli22[14] and Rli33-1.[12,14] Both sRNAs were initially identified in a large-scale tiling array study;[14] Rli22 is an sRNA encoded from the intergenic region of *lmo0028* and *lmo0029* (Fig. 1A) and Rli33-1 is part of a larger transcript designated Rli33. A later study identified 2 individual sRNAs, Rli33-1 and Rli33-2, encoded from the intergenic region of *lmo0671* and *lmo0672* (Fig. 1A).[12]

Based on northern blot analyses, 5′-end mapping via primer extension, and computational predictions of transcription terminator structures, Rli22 and Rli33-1 were estimated to be 105 nt and 121 nt in length, respectively (Figs. S1 and S2). Comparison of the nucleotide sequences of all 7 sRNAs showed that Rli22 and Rli33-1 contain 2 CU-rich regions with homology to the unpaired interhelical region and the apical loop of the Rho-independent terminator of LhrC1-5 (Fig. 1B; Fig. S3). Interestingly, these regions hold the conserved UCCC motif which has been shown to be crucial for the *in vitro* binding of LhrC4 to several target mRNAs (Fig. 1B).[23,24] While LhrC1-5 all contain 3 UCCC motifs situated in unpaired regions (Fig. S3), Rli22 and Rli33-1 hold 2 copies each (Fig. 1C). In Rli22 and Rli33-1, these motifs reside within the apical loop of the large 5′ hairpin structure (hereafter denoted loop A) and the unpaired interhelical region (hereafter denoted the single-stranded stretch; Fig. 1C). Overall, the predicted secondary structures of Rli22 and Rli33-1 slightly differ from LhrC1-5; the 5′-ends of Rli22 and Rli33-1 are more structured than in LhrC1-5, and the sequence and size of the 2 major stems are different (Fig. 1C; Fig. S3).

The striking sequence similarities of the sRNAs prompted us to take a closer look at their individual expression profiles. Similar to LhrC1-5, both Rli22 and Rli33-1 are known to be induced in response to infection-relevant stress conditions. There are, however, slight differences between their patterns of expression (summarized in Table 1). All seven sRNAs were found to be expressed in *L. monocytogenes* exposed to human blood.[14] However, only Rli22 was shown to be expressed in *L. monocytogenes* residing in the intestinal lumen of mice, whereas Rli33 was detected in cells grown to stationary phase.[14] Furthermore, LhrC1-5 were found to be highly induced during intracellular growth in macrophages.[12] Interestingly, the expression of LhrC1-5 occurs in a LisRK-dependent manner upon exposure to the β-lactam antibiotic cefuroxime as well as osmotic stress.[23] To assess whether the expression of Rli22 and Rli33-1 also respond to cefuroxime and osmotic stress, we carried out a northern blot analysis. Furthermore, the promoter activity of *rli22* and *rli33-1* fused to the reporter gene *lacZ* was determined in a β-galactosidase assay. The results from these experiments are shown in Figs. S1 and S2, and summarized in Table 1. Rli33-1 was found to be induced in response to osmotic stress and expression of this sRNA clearly relied on the general stress factor σ^B (Fig. S2). The data showed that the sRNA level varies with the strain background, but the deletion of LhrC1-5 had no effect on Rli33-1 expression (Fig. S2). Conversely, the expression of Rli22 was induced upon cefuroxime exposure in a LisRK-dependent manner (Fig. S1). Interestingly, the yield of Rli22 was significantly higher in a Δ*lhrC1-5* strain

Table 1. Induction profiles of LhrC1-5, Rli22, and Rli33-1. Conditions in which the expression of sRNAs have been reported to be either specifically induced (+) or not induced (−) are shown. ND indicates that the sRNA was not detected in the given study.

Stress condition	LhrC1-5	Rli22	Rli33-1
Intestine	−	+[1]	−
Blood	+[1]	+[1]	+[1]
Intracellular growth in macrophages	+[2]	ND[1]	−/+[$]
Stationary phase	−	−	+[1,#]
β-lactam antibiotics	+[3,¤]	+[4,¤]	−
Osmotic stress (NaCl)/high osmolarity	+[3,¤]	−	+[4,#]

[1]Mraheil et al. [14]
[2]Toledo-Arana et al. [12]
[3]Sievers et al. [23]
[4]This study.
[¤]Expression is LisRK regulated (this study).
[#]Expression is σ^B -dependent (Toledo-Arana et al. [12] and this study).
[$]Was found to be induced both intracellularly and extracellularly by RNA-seq, however, northern blot analysis showed variation in transcript concentrations under these conditions. [12]

relative to the isogenic wild type strain, illustrating a regulatory interconnection between Rli22 and LhrC1-5 (Fig. S1).

Rli22 and Rli33-1 can functionally replace LhrC5 in vivo

Because Rli22 and Rli33-1 contain UCCC motifs also found in LhrC1-5, we tested if these sRNAs would be capable of controlling the expression of LhrC1-5 target mRNAs to the same extent as a single copy of LhrC. In order to compare their regulatory capacity, we generated strains expressing specific sRNAs from the native *lhrC5* promoter, which is strongly activated by LisRK in response to cefuroxime stress.[23] First, a strain lacking all 7 sRNA-encoding genes was constructed (LO28-Δ7). Then, *rli22, rli33-1* or *lhrC5* were fused to the *lhrC5* promoter at the chromosomal locus between *lmo0946* and *lmo0947*. Expression of Rli22, Rli33-1 and LhrC5 from the cefuroxime-inducible *lhrC5* promoter was validated by northern blot analysis. While none of the sRNAs were expressed under non-stressed conditions (Fig. S4), all 3 sRNAs were clearly induced in cells subjected to 1 hour of cefuroxime stress (Fig. 2A and 2B, lanes 2–3). As expected, none of the sRNAs were detected in the LO28-Δ7 strain (Fig. 2A and 2B, lane 1). Next, we tested the levels of *oppA* and *tcsA* mRNAs, which are known to be targeted by LhrC1-5.[24] Upon exposure to cefuroxime, the transcript levels of *tcsA* and *oppA* in strains expressing LhrC5, Rli22 or Rli33-1 were reduced by 2.0- to 2.5-fold relative to the levels detected in the LO28-Δ7 strain (Fig. 2A and 2B; compare lanes 1-3). Thus, when expressed from the *lhrC5* promoter, Rli22 and Rli33-1 affect the transcript levels of *oppA* and *tcsA* to a similar degree as seen for LhrC5.

To address the importance of the conserved UCCC motif for *in vivo* regulation, mutant derivatives encoding Rli22 or Rli33-1 with nucleotide substitutions in either loop A (mut_loopA), the single-stranded stretch (mut_ss), or both (double_mut), were included in the analysis (Fig. 1C). The mutations were designed to preserve the secondary structure of the sRNAs. For Rli22, mutation of either the loop A or the single-stranded region had a minor effect on *tcsA* expression, but was still able to strongly decrease the yield of *oppA* (Fig. 2A, lane 4 and 5). In contrast, the yields of both mRNA targets were enhanced in the strain expressing the Rli22 double mutant (Fig. 2A, lane 6). In the case of Rli33-1, the levels of *tcsA* and *oppA* mRNA were clearly enhanced in all mutant strains compared to the strain expressing the wild type Rli33-1 (Fig. 2B, lane 4-6). Taken together, the RNA gel blot analysis indicates that mutations of both UCCC motifs in Rli22 or Rli33-1 alleviate the effect of the sRNAs on the steady-state levels of the mRNA targets, signifying that the UCCC motifs are important for *in vivo* repression. However, northern blot analysis of the sRNA variants also showed that the yields of some of the mutated sRNAs were altered (Fig. 2). The yields of the Rli22 loop A mutant and double mutant were similar to wild type Rli22 (1.13 and 0.98 relative to wild type; compare lane 3 to lanes 4 and 6 in Fig. 2A), whereas the level of the Rli22 single-stranded mutant was slightly decreased (0.72; compare lanes 3 and 5). For Rli33-1, the steady-state levels of all 3 mutant variants were lower relative to wild type (0.60, 0.39 and 0.33; compare lane 3 to lanes 4-6 in Fig. 2B). These variations should be taken into account when evaluating the regulatory effect of the individual sRNAs.

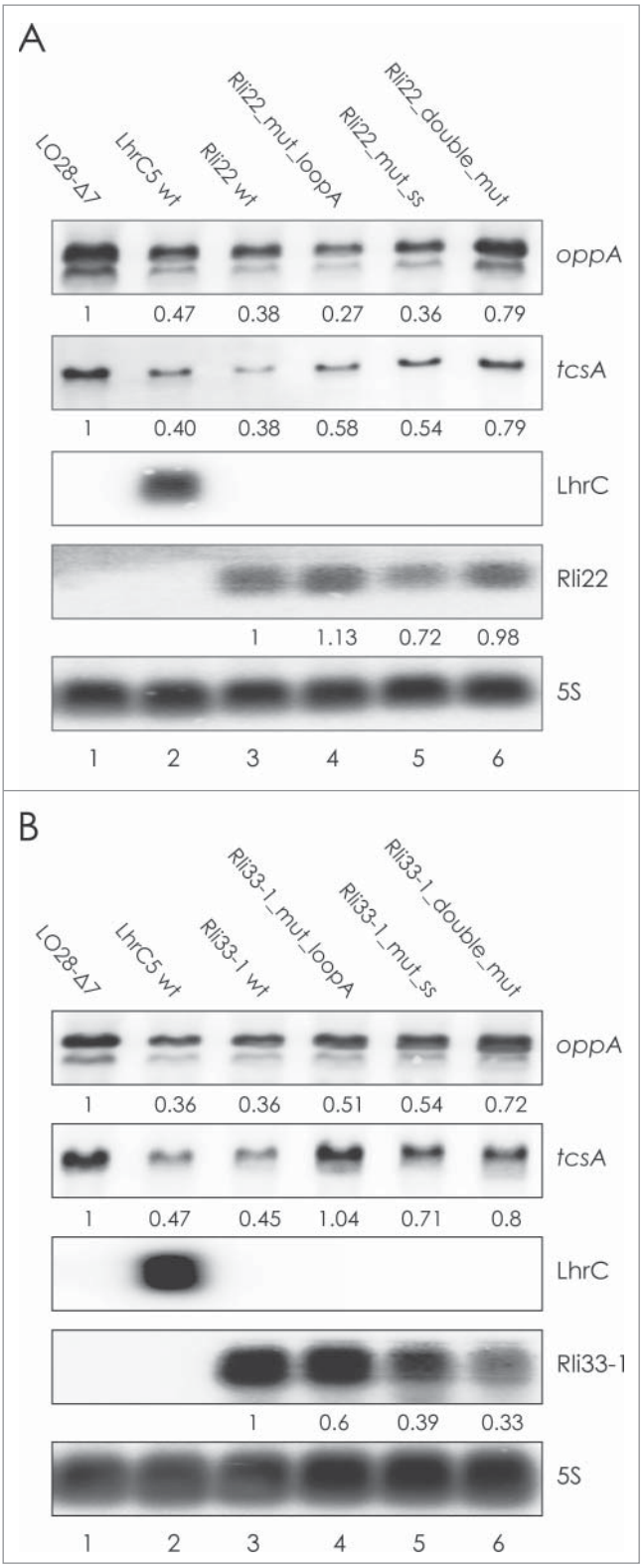

Figure 2. Rli22 and Rli33-1 are able to functionally replace LhrC5 *in vivo*. The ability of Rli22 (A) and Rli33-1 (B) to regulate LhrC target genes *in* vivo was investigated by northern blot analysis. A strain lacking all sRNA-encoding genes (LO28-Δ7, lane 1) and strains expressing either LhrC5 (lane 2), Rli22/Rli33-1 wt (lane 3) or mutant Rli22/Rli33-1 (lanes 4-6) from the *lhrC5* promoter were subjected to cefuroxime stress for 1 hour to induce expression of the sRNAs. Northern blots were probed for *tcsA* mRNA, *oppA* mRNA, LhrC, Rli22, Rli33-1, and 5S (loading control). The levels of *oppA* and *tcsA* mRNA (normalized to 5S) encoded in the strains tested relative to the LO28-Δ7 strain, are shown in black below lanes 1 to 6. Below the sRNA bands, the levels of Rli22/Rli33-1 (normalized to 5S), relative to wt Rli22/Rli33-1, are depicted in black. The experiment was repeated 3 times with similar results.

In the case of Rli33-1 the increased mRNA levels in the mutant strains might be due to mutations of the UCCC motifs as well as altered sRNA yields relative to wild type Rli33-1, whereas for Rli22 the increased mRNA levels of the mutant variants are clearly a result of disrupting the UCCC motifs of this sRNA.

Using a reporter gene fusion strategy, it was previously demonstrated that LhrC1-5 control expression of *oppA, tcsA* and *lapB* at the post-transcriptional level.[23,24] For this approach, sequences ranging from the transcriptional start sites into the first codons of either *tcsA, oppA*, or *lapB* were fused downstream of a moderate promoter (known to be insensitive to LhrC regulation), in-frame to *lacZ* in the translational reporter vector pCK-lac.[23,24] In the present study, the reporter gene strategy was implemented to evaluate the regulatory effect of Rli22, Rli33-1 and LhrC5 on *oppA, tcsA* and *lapB*. In Fig. 3A-F and Fig. S5, we present the results of the β-galactosidase assays for each plasmid construct in the strain lacking all 7 sRNAs (LO28-Δ7), or strains expressing LhrC5, Rli22 or Rli33-1. Under non-stress conditions, no difference in the relative β-galactosidase activity was observed (Fig. S5). As expected, the β-galactosidase activity was significantly lower in the strain expressing LhrC5 compared to the strain lacking all 7 sRNA-encoding genes (Fig. 3A–F). Interestingly, upon expression of the wild type variants of Rli22 (Fig. 3A–C) and Rli33-1 (Fig. 3D–F), the β-galactosidase activity was reduced to the same extent as seen for LhrC5, corresponding to a fine-tuning effect. The mutant variants of Rli22 and Rli33-1 were also evaluated using the reporter fusion strategy. For strains encoding single-mutant versions of Rli22 (i.e. mutated loop A or single-stranded stretch), the expression from *tcsA-lacZ* was significantly higher compared to the strain encoding wild type Rli22, whereas only Rli22_mut_ss showed a reduced regulatory effect on expression from *lapB-lacZ* (Fig. 3B–C). For *oppA-lacZ*, expression was unaffected by the single-mutant versions of Rli22 (Fig. 3A). For Rli33-1, mutation of either of the UCCC motifs reduced the regulatory effect on the expression from *lapB-lacZ* (Fig. 3F). However, only mutation of the loop A region, and not the single-stranded stretch, reduced the regulatory effect on *oppA* and *tcsA* (Fig. 3D–E). Finally, for strains encoding Rli22 or Rli33-1 mutated in both UCCC motifs, the regulatory effect on all 3 fusions was significantly reduced; notably, the β-galactosidase activity of the strains encoding the double mutant variants was equal to the activity of the LO28-Δ7 strain (Fig. 3A–F). The results of the β-galactosidase assays are well-correlated with the northern blot experiments illustrating the effects of the mutations of sRNAs on the steady-state levels of the mRNA targets.

Taken together, our data demonstrate that Rli22 and Rli33-1 are able to inhibit the expression of *tcsA, oppA* and *lapB* at the post-transcriptional level to a similar extent as LhrC5. Furthermore, the regulatory effect involves the 5′-ends of the target mRNAs as well as the conserved UCCC motifs of Rli22 and Rli33-1, although the 2 UCCC motifs are not strictly equivalent for regulation.

Rli33-1 and Rli22 are able to bind LhrC target mRNAs in vitro

Our data strongly suggested that Rli33-1 and Rli22 control the expression of *oppA, tcsA and lapB* at the post-transcriptional level by a direct binding to the mRNAs. Given the fact that Rli22 and Rli33-1 contain the same UCCC motif also held by LhrC1-5, we postulate that all these sRNAs regulate the target genes by a similar mechanism. Using IntaRNA,[34,35] we predicted that Rli22 and Rli33-1 could bind to the AG-rich SD regions of *lapB* and *oppA* mRNA (Fig. S6), corresponding to the regions shown to interact with LhrC1-5.[23,24] In the case of *tcsA* mRNA, LhrC1-5 have been predicted to bind upstream of the SD region (−96 to −87, relative to the translational start site),[24] while Rli22 and Rli33-1 were predicted to bind the SD region of this mRNA (from −15 to +1 and from −15 to +4, respectively; Fig. S6). In all cases, the *in silico* predictions involved the CU-rich regions of Rli22 and Rli33-1. The *tcsA* and *lapB* mRNAs were predicted to interact with the CU-rich region within the single-stranded stretches of both sRNAs. For *oppA* mRNA, Rli22 was expected to bind via the CU-rich single-stranded stretch, whereas for Rli33-1, the strongest predicted interaction was with the loop A site.

In order to monitor the formation of complexes between the sRNAs and mRNAs, electrophoretic mobility shift assays (EMSA) were performed (Fig. 3G–J). 5′-end labeled Rli22 and Rli33-1 were mixed with increasing concentrations of unlabeled *oppA, lapB* or *tcsA* RNA. Both Rli22 and Rli33-1 bound *oppA* RNA effectively with nearly all of the labeled sRNA being shifted in the presence of only a 5-fold excess of the mRNA (Fig. 3G and 3I). For both sRNAs, 2 shifted bands appeared with increasing concentrations of *oppA* RNA, indicating that 2 *oppA* molecules bind to a single sRNA molecule. In contrast, high concentrations of *lapB* mRNA resulted in a single prominent shift in the case of Rli33-1 (Fig. 3J), whereas for Rli22, 2 weaker bands were observed (Fig. 3H). This suggests that both sRNAs are able to bind *lapB* mRNA *in vitro*, but the nature of their interactions may differ. Surprisingly, no interaction could be detected between *tcsA* RNA and Rli22 or Rli33-1 (Fig. S7). Because the ribosome binding site of *tcsA* mRNA is predicted to be sequestered into a hairpin structure (Fig. S8), the RNA was annealed to Rli22 and Rli33-1 at high temperature followed by slow cooling to 37°C. As a positive control, a complex with 5′-end labeled LhrC4, which has previously been shown to bind *tcsA* RNA *in vitro*,[24] was formed. The data showed that under the conditions used in this study, Rli22 and Rli33-1 are not able to form stable complexes with *tcsA* RNA *in vitro* (Fig. S7). Given the observed sRNA-dependent control of *tcsA in vivo*, we speculate that the regulatory effect exerted by Rli22 and Rli33-1 might rely on the presence of one or more *trans*-acting co-factors. Because LhrC was originally identified by Hfq co-immunoprecipitation,[15] we investigated whether Rli22 and Rli33-1 interact with this co-factor as well, using EMSAs conducted with increasing concentrations of purified *Listeria* Hfq protein and 5′-end labeled sRNAs. LhrC4, which is known to bind
Hfq *in vitro*, was included as a positive control. Under the conditions used in this *in vitro* binding study, neither Rli22 nor Rli33-1 was able to bind Hfq (Fig. S7).

Overall, the EMSAs indicate that the 5′ untranslated regions (UTR) of the *oppA* and *lapB* mRNAs are direct targets of Rli22 and Rli33-1. In contrast, no evidence for direct binding of Rli22 and Rli33-1 to *tcsA* RNA *in vitro* was observed, indicating that additional factors are needed for Rli22 and Rli33-1 to exert

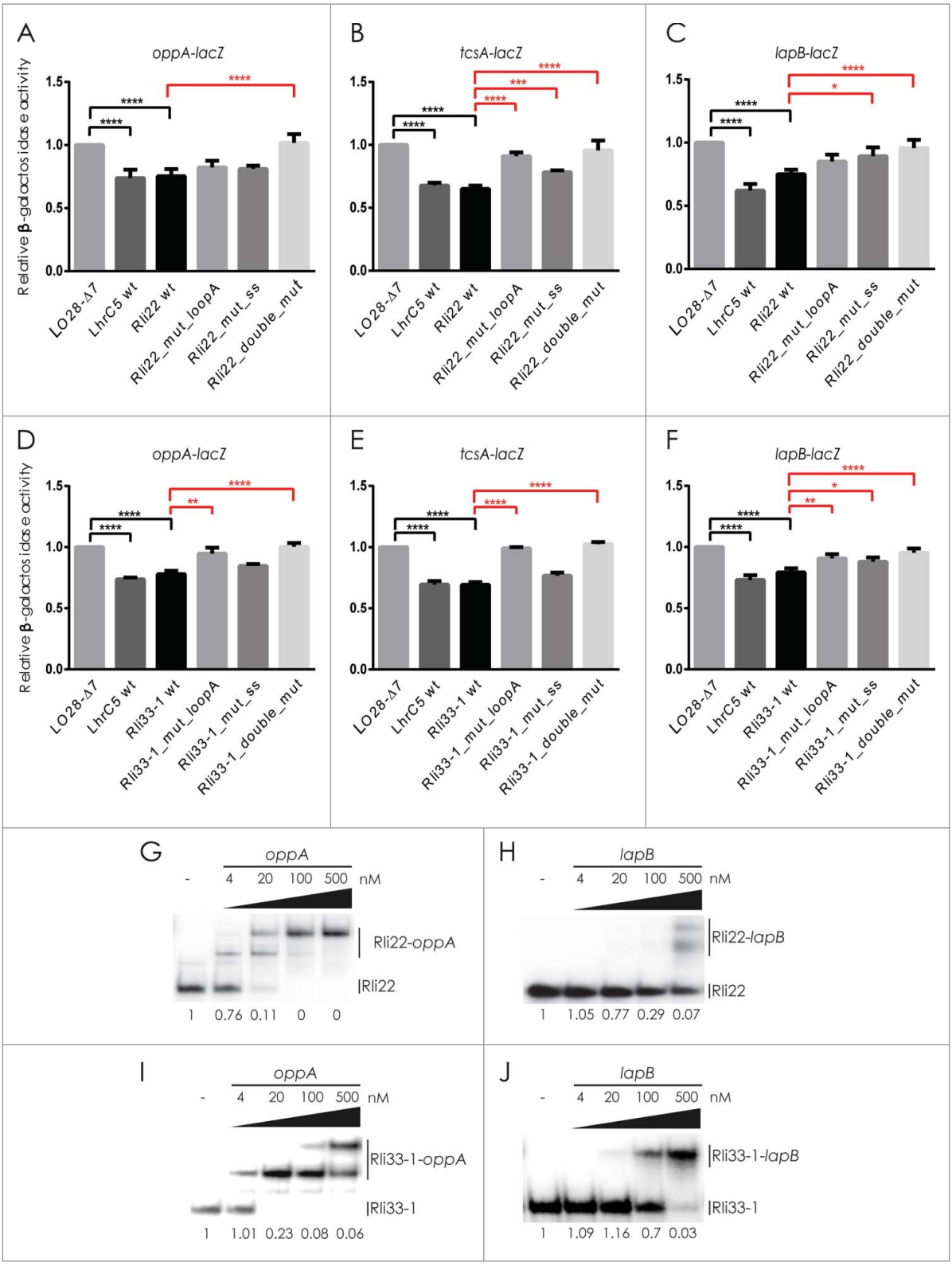

Figure 3. Rli22 and Rli33-1 regulate LhrC target genes at the post-transcriptional level. The ability of Rli22 (A–C) and Rli33-1 (D–F) to regulate LhrC target genes was analyzed in β-galactosidase assays. An LO28-Δ7 strain and strains expressing wild type or mutant sRNA variants—each carrying a translational reporter gene fusion of either *oppA, tcsA*, or *lapB* to *lacZ*—were exposed to a subinhibitory concentration of cefuroxime (4 μg/ml) for 3 hours. Results are the average of 3 biological replicates each conducted in technical duplicates. Four black asterisks indicate a significant decrease in relative β-galactosidase activity compared to the LO28-Δ7 strain with $P < 0.0005$. Relative β-galactosidase activities significantly different from the Rli22/Rli33-1 wt strain are marked with red asterisks (2: $P < 0.005$, 3: $P < 0.001$ and 4: $P < 0.0005$). (G–J) electrophoretic mobility shift assays (EMSA) of sRNA-mRNA interactions. 4 nM of 5′-end labeled Rli22 (G–H) or Rli33-1(I–J) was incubated with increasing concentrations of unlabeled *oppA* RNA or *lapB* RNA. The fraction of unbound sRNA is shown below each lane. The experiment was repeated 3 times with similar results.

their regulatory effect on *tcsA*. Based on the strong binding affinity of both sRNAs to *oppA* RNA, we chose this target gene for further analysis of the mechanism underlying the observed regulatory effects of Rli22 and Rli33-1.

Binding of Rli22 and Rli33-1 to the SD region of oppA *mRNA relies on 2 conserved UCCC motifs*

The observations made so far suggest that Rli22 and Rli33-1 act by binding to the SD region of *oppA* mRNA. Therefore, the importance of this region for the *in vitro* interaction was investigated by EMSA using 5′-end labeled sRNA and either unlabeled *oppA* RNA (*oppA*_wt) or a mutant version (*oppA*_mut) containing substitutions of 3 nucleotides in the SD region (Fig. 4A). Mutation of *oppA* (5′GGGA to 5′CGCU) fully disrupted complex formation with wild type Rli22 (Fig. 4B–D, left), indicating that the SD region of *oppA* is important for the interaction with Rli22. The importance of each of the UCCC motifs of Rli22 was investigated using mutant variants of this sRNA. Three nucleotide substitutions (5′UCCC to 5′AGCG) were introduced into the CU-rich regions of loop A (Rli22_mut_loopA) and the single-stranded stretch (Rli22_mut_ss; Fig. 4A). The mutations were designed to avoid changes in the secondary structure of the sRNA and to restore basepairing with the *oppA* mutant (*oppA*_mut). For both Rli22 single mutants, the addition of wild type *oppA* RNA resulted in a single complex; the second one was either weak or not formed at all (Fig. 4B and 4C, right). Thus, disruption of one of the UCCC motifs in Rli22 prevents binding of a second *oppA* transcript to the sRNA. We also tested whether the Rli22 single mutants were capable of interacting with the complementary *oppA*_mut variant (Fig. 4B and 4C, right). A single complex was clearly visible for both Rli22_mut_loopA and Rli22_mut_ss. We finally tested the binding of the Rli22 variant mutated in both UCCC motifs (Rli22_double_mut; Fig. 4D, right). No binding was observed between Rli22_double_mut and *oppA*_wt; however, when incubated with *oppA*_mut, the interaction with the mutated version of Rli22 was fully restored. Similar experiments were carried out for Rli33-1 (Fig. 5A–D). As for Rli22, Rli33-1_wt was not able to bind *oppA*_mut, indicating that the SD region is the target sequence (Fig. 5B-D, left). Interestingly, mutation of the loop A region of Rli33-1 prevented complex formation with wild type *oppA*, but the interaction was restored when Rli33-1_mut_loopA was incubated with *oppA*_mut (Fig. 5B, right). This suggests that the loop A region of Rli33-1 is the main contributor to *oppA* mRNA binding. For Rli33-1_mut_ss, a single complex was formed in the presence of wild type *oppA*, whereas no complex was detected when incubated with *oppA*_mut (Fig. 5C, right). This result indicates that the interaction between the CU-rich single-stranded stretch in Rli33-1 and *oppA* is relatively weak. With respect to Rli33-1 mutated in both UCCC motifs (Rli33-1_double_mut), binding to *oppA*_wt was disrupted (Fig. 5D, right). Addition of *oppA*_mut to Rli33-1_double_mut, however, led to a band shift pattern similar to the one of *oppA*_wt and Rli33-1_wt (Fig. 5D). These experiments revealed some differences in how Rli22 and Rli33-1 bind to *oppA* mRNA. For Rli22, the 2 UCCC motifs appear to be equally important for binding of *oppA* mRNA, whereas for Rli33-1 the UCCC motif in the Loop A region is clearly the most important site of interaction.

To further delineate the binding sites, the interaction between the sRNAs and *oppA* RNA were probed using various enzymes. The 5′-end labeled Rli22 and Rli33-1 were subjected to RNase hydrolysis in the absence and presence of *oppA* RNA (Fig. 6A and 7A; Fig. S9). Cleavages were induced by RNases V1 (specific for double-stranded regions), RNase T1 (specific for unpaired guanine) and RNase T2 (preference for unpaired adenines). The cleavage patterns obtained for both sRNAs are well-correlated with the proposed secondary structure models (Fig. 1C; Fig. 6B and 7B). Indeed, the strongest single-strand specific cleavages were observed in the apical loops and the single-stranded stretch while RNase V1 cuts were found in the 2 major stems. For Rli22, binding of *oppA* RNA induced protection of the 2 distant regions containing the UCCC motif (Fig. 6; Fig. S9A). Complex formation led to a prominent protection of the residues in the loop A region (C25-U34) against RNase T2 as well as protection of G37 against RNase T1. Concomitantly, protection against RNase V1 was observed at U19. At the same concentrations of *oppA* RNA, nucleotides located in the single-stranded stretch of Rli22 were also protected from RNase T1 and T2 cleavages, while weak RNase V1 cuts appeared at position 74 and 75. Very similar foot-printing data was observed for Rli33-1. The two regions containing the UCCC motifs were protected upon addition of *oppA* RNA (Fig. 7; Fig. S9B). However, protection of the loop A region in Rli33-1 (U28-U37) appeared at a lower concentration of *oppA* RNA than for the protections observed in the single-stranded stretch, confirming that loop A is the predominant site of interaction with *oppA* RNA.

To investigate the extent of sRNA binding to *oppA* mRNA, a foot-printing analysis was performed using dimethyl sulfate (DMS), which methylates adenines at N1 and cytosines at N3. The positions and reactivities of the modified residues were detected by reverse transcription (RT; Figs. 8 and 9). A secondary structure model for the 5′ UTR of *oppA* was proposed based on the DMS reactivities. In this structure, the adenines surrounding the SD region of *oppA* RNA was highly reactive toward DMS. Binding of Rli22 resulted in a strong RT pause located just before the SD sequence (Fig. 8A–B). In addition, protection against DMS modifications was restricted to a stretch of adenines located just upstream from the SD region, which is complementary to the CU-rich regions of Rli22 (−20 to −15 relative to the translational start site). To evaluate the individual binding mechanism of each CU-rich region, *oppA* RNA was incubated with either Rli22_mut_loopA or Rli22_mut_ss. Similar to wild type Rli22, the Rli22_mut_ss variant caused an RT pause accompanied by protection of the adjacent adenines. For Rli22_mut_loopA, *oppA* induced the same protection of the stretch of adenines against DMS, although the RT pause at the SD region was less prominent. When mutating both UCCC motifs of Rli22, the RT pause and local protection of the SD region was no longer observed, substantiating that loop A and the single-stranded stretch of Rli22 are the only sites of interaction with *oppA* mRNA. Similar experiments were carried out for Rli33-1 (Fig. 9A–B). In the presence of wild type Rli33-1, a very strong RT pause was

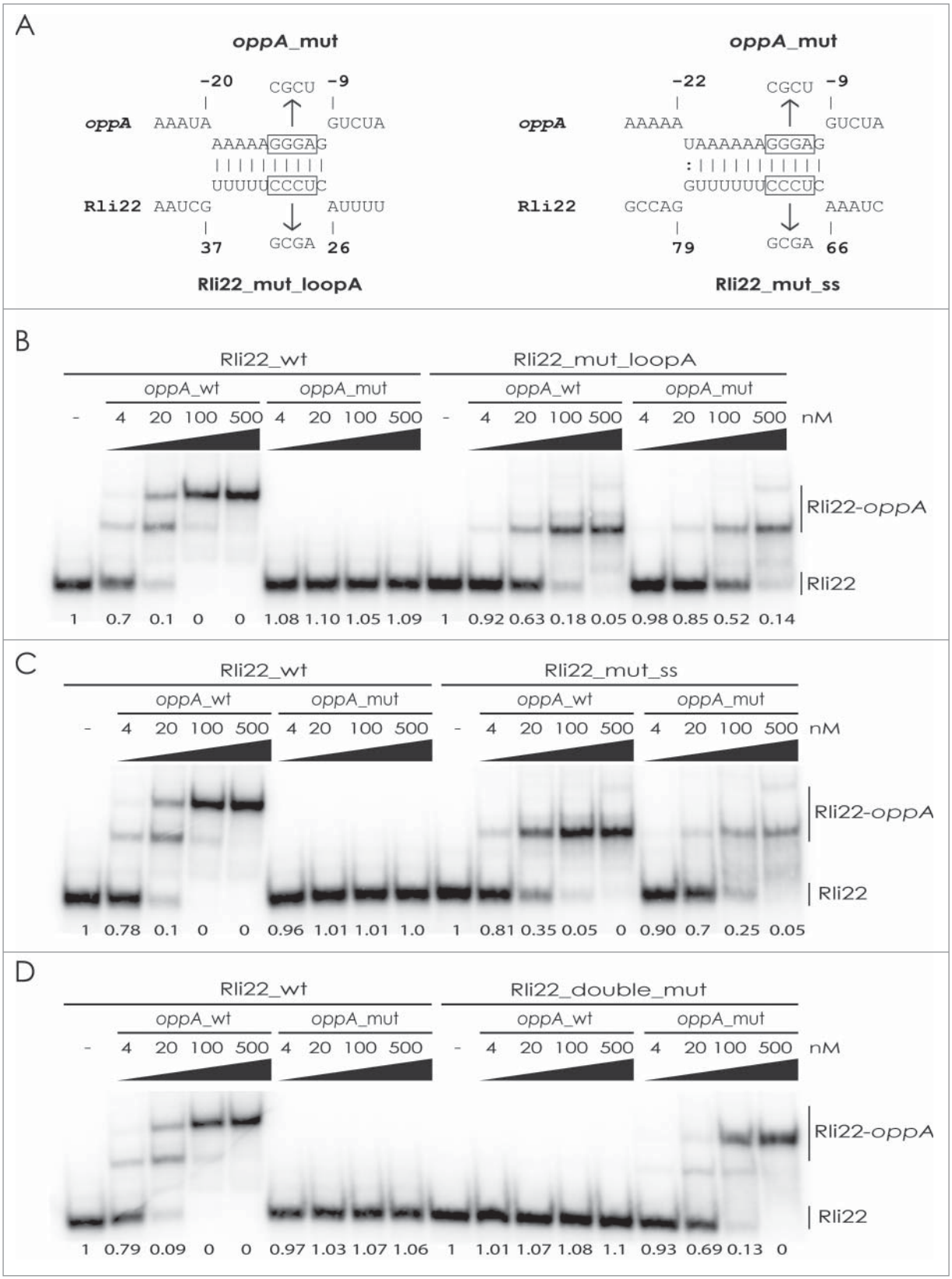

Figure 4. Interaction with *oppA* mRNA involves both CU-rich regions of Rli22. The interaction between Rli22 and *oppA* mRNA was investigated by EMSA. (A) Predicted interactions between the SD region of *oppA* mRNA and the CU-rich regions of Rli22. Nucleotide substitutions were introduced in the UCCC motifs (boxed) of Rli22 or the complimentary GGGA sequence in *oppA* (boxed). Sequences of Rli22_mut_loopA, Rli22_mut_ss and *oppA*_mut are shown. The double mutant of the sRNA (Rli22_double_mut) contains the nucleotide substitutions of both mut_loop and mut_ss. For the EMSA experiments, 4 nM of 5′-end labeled Rli22_wt and mutant variants Rli22_-mut_loopA (B), Rli22_mut_ss (C) or Rli22_double_mut (D) were incubated with increasing concentrations of unlabeled *oppA*_wt or *oppA*_mut. The fraction of unbound sRNA is indicated below each lane. The experiment was repeated 3 times with similar results.

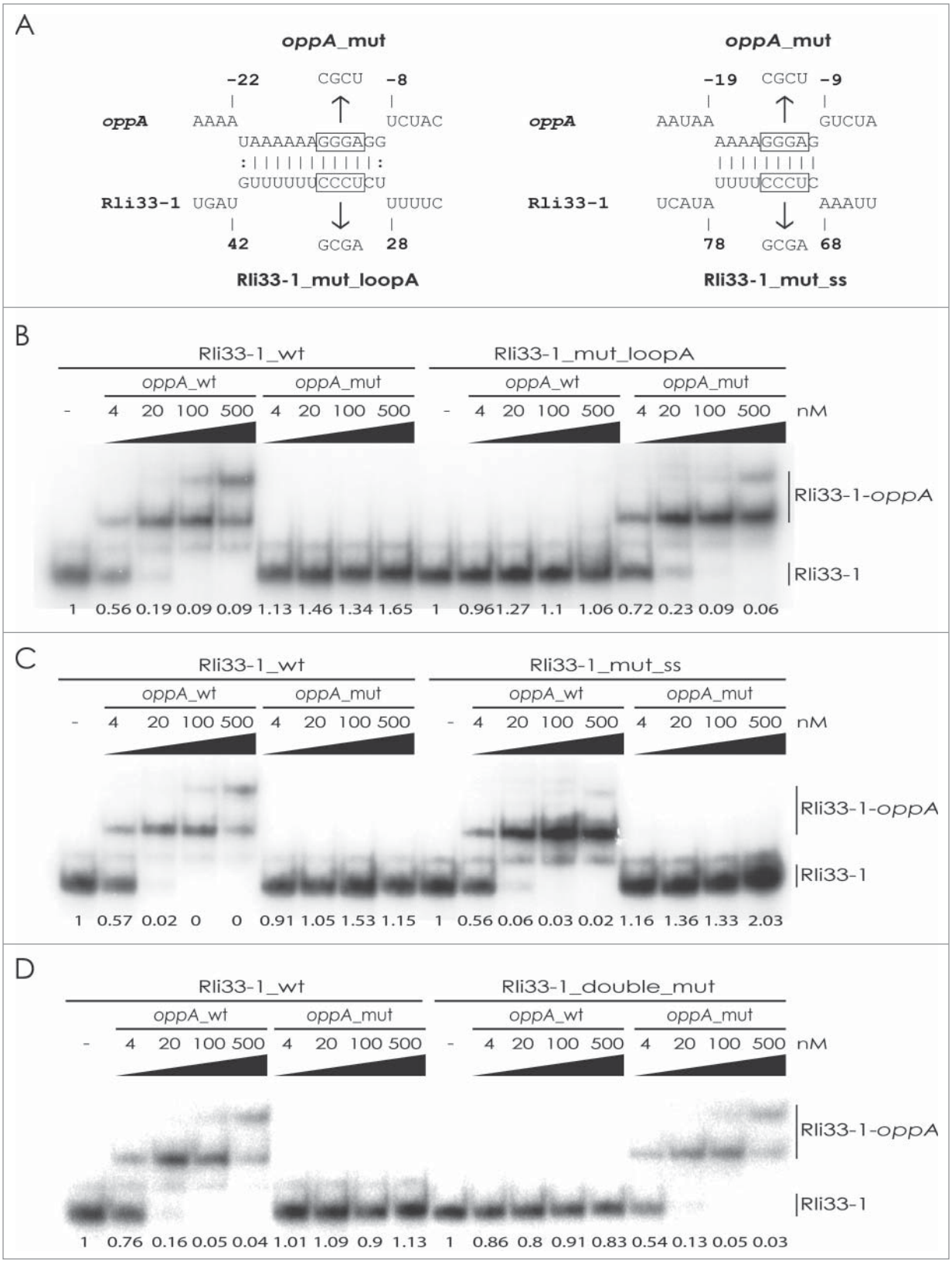

Figure 5. The Loop A region of Rli33-1 is the primary site of interaction with *oppA*. The interaction between Rli33-1 and *oppA* mRNA was investigated by EMSA. (A) Predicted interactions between the SD-region of *oppA* mRNA and the CU-rich regions of Rli33-1. For Rli33-1, mutant variants carry nucleotide substitutions in the UCCC motif (boxed) of either the loop A region (Rli33-1_mut_loopA), the ss region (Rli33-1_mut_ss) or both regions (Rli33-1_double_mut). For the EMSA experiments, 4 nM of 5′-end labeled Rli33-1_wt and 5′-end labeled mutants variants Rli33-1_mut_loopA (B), Rli33-1_mut_ss (C) or Rli33-1_double_mut (D) were incubated with increasing concentrations of unlabeled *oppA*_wt or *oppA*_mut. The fraction of unbound sRNA is indicated below each lane. The experiment was repeated 3 times with similar results.

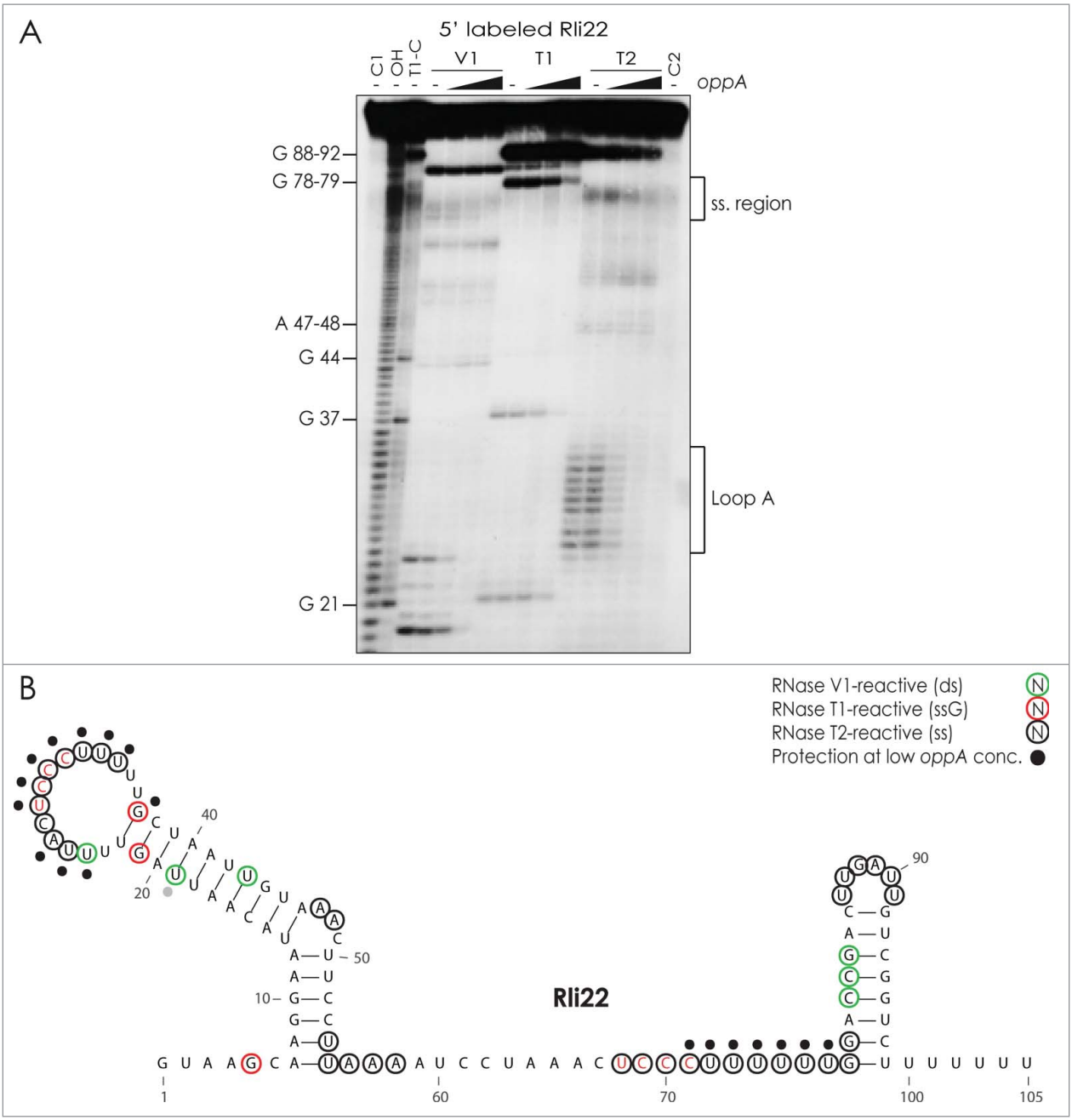

Figure 6. The *oppA* mRNA protects both CU-rich regions of Rli22. (A) Enzymatic probing of the interaction between Rli22 and *oppA* mRNA. 5′-end labeled sRNA was treated with RNase V1 (5 min), T1 (5 min) or T2 (10 min) in either the absence (−) or presence of increasing concentrations of *oppA* RNA (to an excess amount of 125 fold). To serve as controls, untreated sRNA (C1, C2), an alkaline ladder (OH^-) and RNase T1 ladder (T1-C) were included. The experiment was repeated 3 times with similar results. The result from an experiment in which the gel run time was increased to obtain a better separation of the single-stranded region is presented in Fig. S9A. (B) Secondary structures of Rli22 illustrating the cleavage pattern upon binding to *oppA* mRNA. Residues cleaved by RNase V1 (green), RNase T1 (red) or RNase T2 (black) are encircled. Residues of Rli22 that appeared protected at low concentration of *oppA* RNA are indicated with black dots.

observed at the SD region of *oppA* RNA, which made the local protection of the upstream stretch of adenines less detectable. For *oppA* RNA incubated with Rli33-1_mut_ss, the RT pause and foot-print were identical to those caused by Rli33-1_wt. In contrast, upon mutation of the loop A site of Rli33-1 the protections were located at fewer adenines upstream of the SD sequence and the RT pause was absent (Fig. 9A–B). For Rli33-1_double_mut, binding of *oppA* RNA was completely disrupted, illustrated by the lack of both the RT pause and foot-print of the upstream region. These results suggest that both CU-rich regions of Rli33-1 are able to bind *oppA* mRNA independently of each other. However, the 2 sites are not strictly equivalent; Loop A contains the preferred binding site of Rli33-1.

Collectively, structure probing confirmed that the interaction of Rli22 and Rli33-1 with *oppA* mRNA relies on the UCCC motifs of the sRNAs and the SD region of the mRNA (Figs. 8C and 9C). Both CU-rich regions of Rli22 and Rli33-1 are able to bind *oppA* mRNA, demonstrating that 2 conserved regions of the sRNAs recognize a single region on the mRNA. Furthermore, the results support the notion that the sRNAs interact with *oppA* mRNA in slightly different ways: while the 2

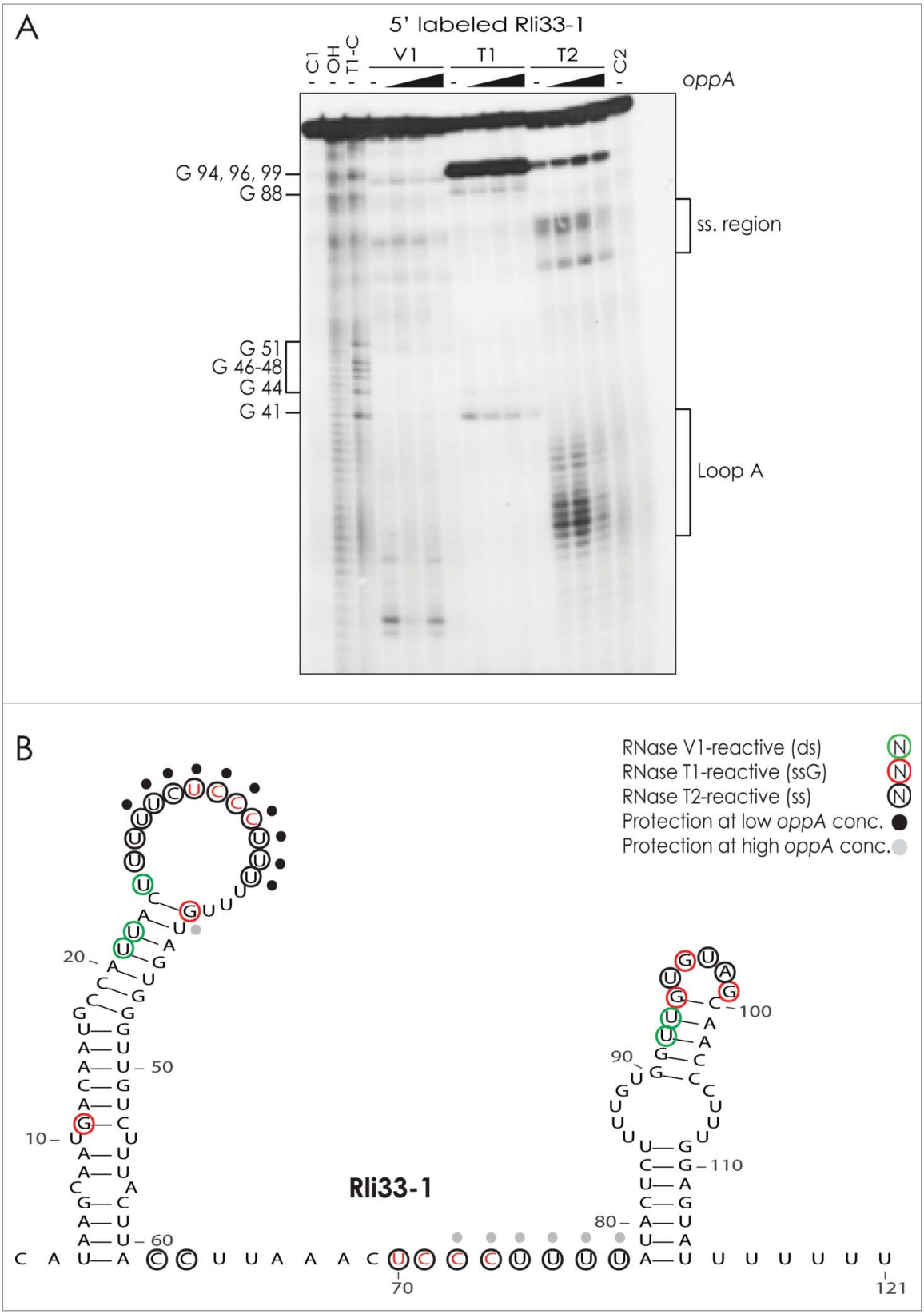

Figure 7. The *oppA* mRNA protects both CU-rich regions of Rli33-1. (A) Enzymatic probing of the interaction between Rli33-1 and *oppA* mRNA. 5′-end labeled sRNA was treated with RNase V1 (5 min), T1 (5 min) or T2 (10 min) in either the absence (—) or presence of increasing concentrations of *oppA* RNA (to an excess amount of 125 fold). To serve as controls, untreated sRNA (C1, C2), an alkaline ladder (OH^-) and RNase T1 ladder (T1-C) were included. The experiment was repeated 3 times with similar results. The result from an experiment featuring a better separation of the single-stranded region is presented in Fig. S9B. (B) Secondary structures of Rli33-1 illustrating the cleavage pattern upon binding to *oppA* mRNA. Residues cleaved by RNase V1 (green), T1 (red) or T2 (black) are encircled. Residues of Rli33 that appeared protected at high concentration of *oppA* RNA are indicated with gray dots. All other protected residues, marked by black dots, appeared at a low concentration of *oppA*.

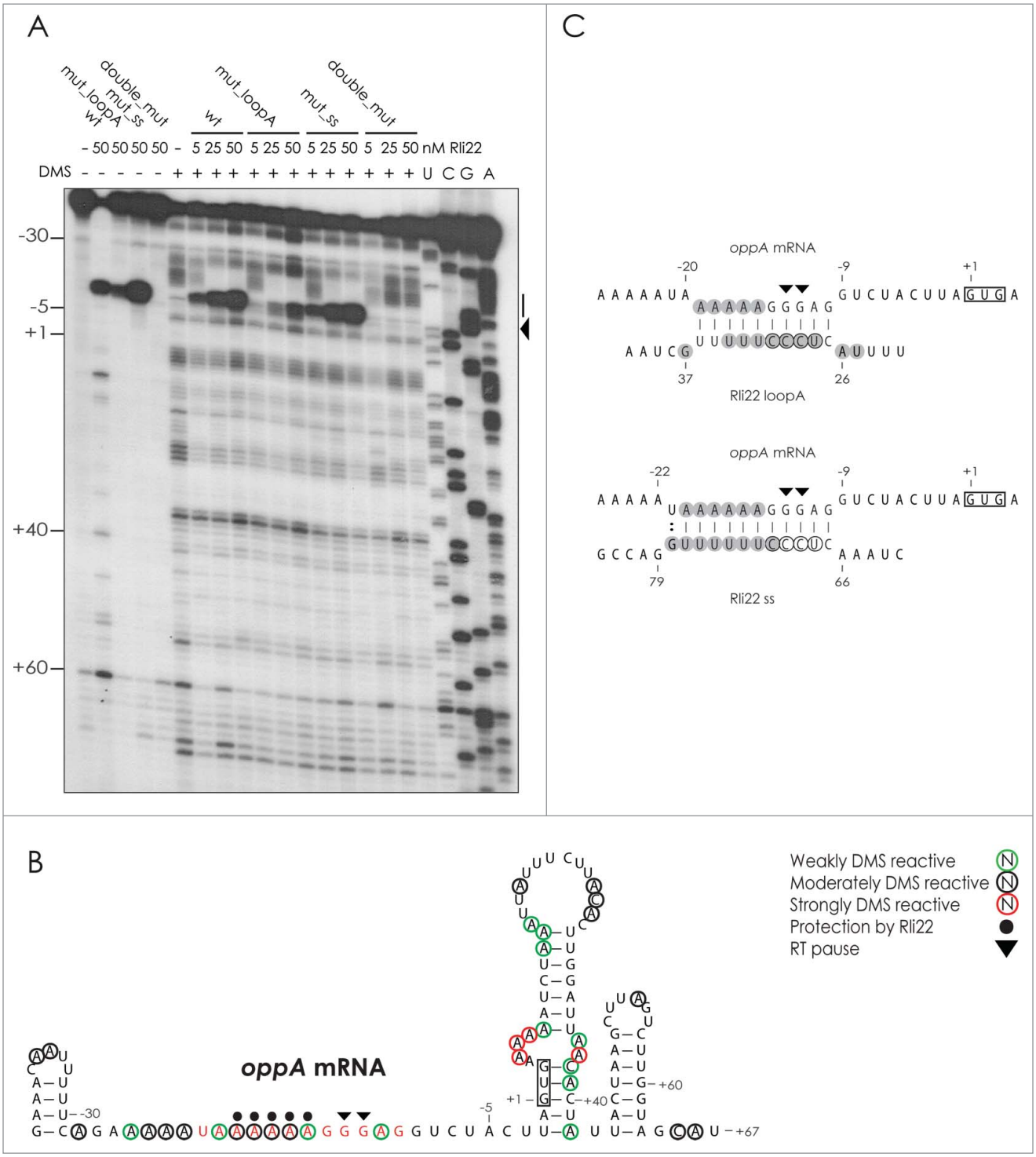

Figure 8. Both CU-rich regions of Rli22 target the SD region of *oppA* mRNA. (A) DMS foot-printing of *oppA* RNA in the absence or presence of Rli22. Unlabeled *oppA* transcript was incubated with increasing concentrations of wild type sRNA or mutant variants (to an excess amount of 5-fold) and treated with DMS followed by reverse transcription of *oppA*. Translational start site (+1), RT pauses (arrow) and protection from DMS (black line) induced by sRNA-binding are indicated. The experiment was repeated 3 times with similar results. (B) Secondary structure of *oppA* RNA illustrating DMS reactivity pattern in the absence and presence of Rli22. Encircled nucleotides signify nucleotides reactive toward DMS. Black circles indicate protection induced by the presence of Rli22, while arrows indicate RT pauses caused by sRNA binding. The SD region of *oppA* mRNA, to which Rli22 is predicted to bind is highlighted in red. The start codon is boxed, and translational start site is indicated (+1). For Rli22, the single-mutations in the sRNA did not alter the footprint. (C) Predicted interactions of the SD region of *oppA* mRNA and the CU-rich regions of Rli22. The results from structure probing experiments of the interactions between Rli22 and *oppA* RNA are summarized: gray circles indicate nucleotides for which a protection, due to RNA binding, was observed; black arrows signify RT pauses induced by sRNA binding. Conserved UCCC motifs in Rli22 are marked with black circles. The translational start codon of *oppA* mRNA is boxed.

CU-rich sites of Rli22 are equivalent, the loop A site of Rli33-1 is clearly the preferred binding site for *oppA* mRNA. Finally, none of the sRNAs were able to induce long distance changes, which indicates that Rli22 and Rli33-1 binding occurs solely at the SD region, only locally affecting the secondary structure of *oppA* mRNA.

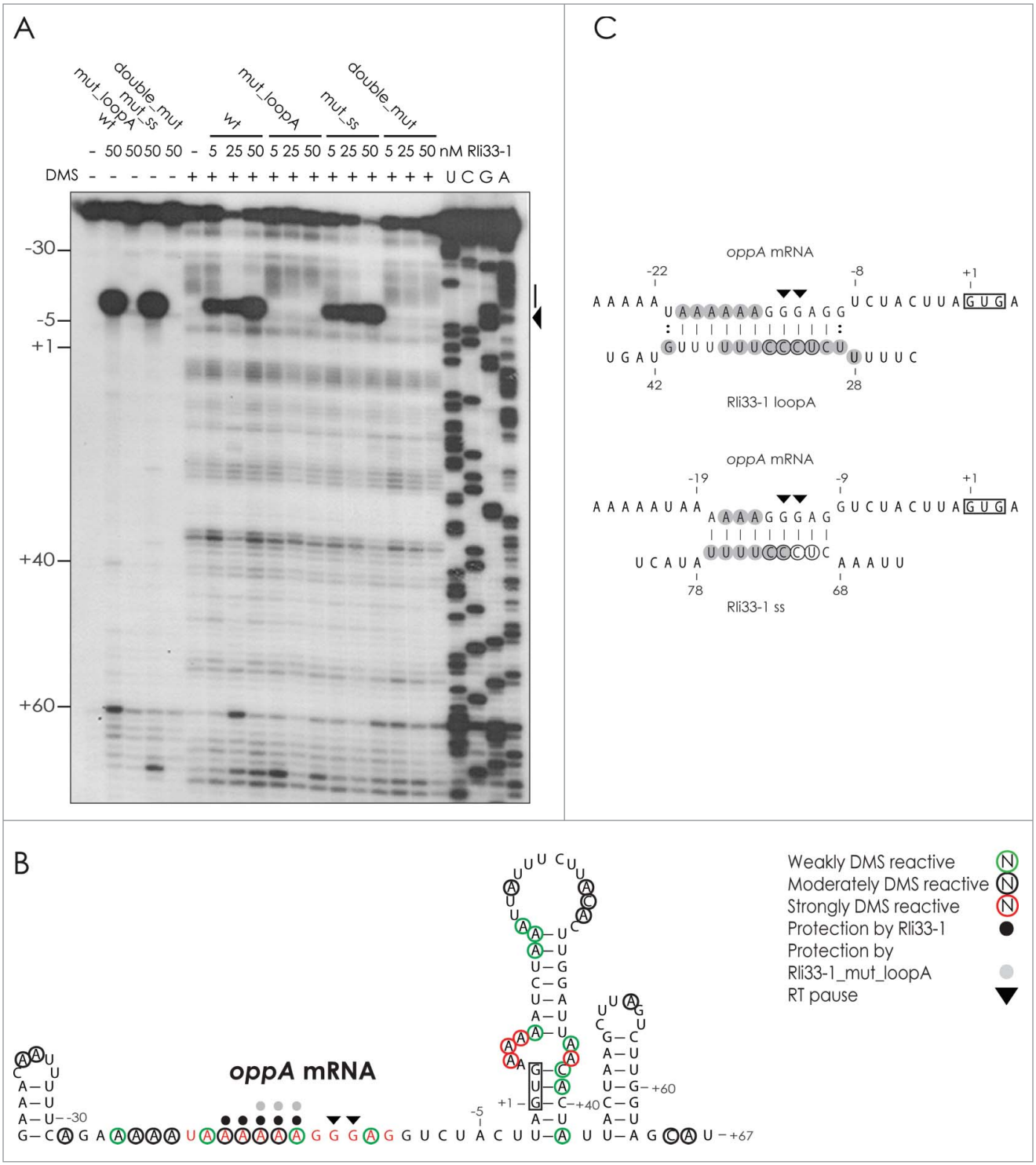

Figure 9. Rli33-1 mutated in Loop A exerts less protection of the SD region of *oppA* mRNA. (A) DMS foot-printing of *oppA* RNA in the absence or presence of Rli22. Unlabeled *oppA* transcript was incubated with increasing concentrations of wild type sRNA or mutant variants (to an excess amount of 5-fold) and treated with DMS followed by reverse transcription of *oppA*. Translational start site (+1), RT pauses (arrow) and protection from DMS (black line) induced by sRNA-binding are indicated. The experiment was repeated 3 times with similar results. (B) Secondary structure of *oppA* RNA illustrating DMS reactivity pattern in the absence and presence of Rli33-1. Encircled nucleotides signify nucleotides reactive toward DMS. Black and gray circles indicate protection induced by the presence of Rli33-1, while arrows indicate RT pauses caused by sRNA binding. The SD region of *oppA* mRNA, to which Rli33-1 is predicted to bind is highlighted in red. The start codon is boxed, and translational start site is indicated (+1). Mutation in loop A revealed less protected adenines while the foot-print remained identical to the wild type for Rli33-1 mutated in the single-stranded region (C) Predicted interactions of the SD region of *oppA* mRNA and the CU-rich regions of Rli33-1. The results from structure probing experiments of the interaction between Rli33-1 and *oppA* RNA are summarized: Gray circles indicate nucleotides, for which a protection due to RNA binding was observed; black arrows signify RT pauses induced by sRNA binding. The conserved UCCC motifs in Rli33-1 are encircled in black, and the translational start codon of *oppA* mRNA is boxed.

The UCCC motifs of Rli22 and Rli33-1 prevent ribosomal binding to oppA *mRNA*

The results obtained so far indicate that Rli22 and Rli33-1 down-regulate *oppA* expression through an antisense mechanism. Accordingly, we expect that binding of Rli22 and Rli33-1 to the SD region of *oppA* mRNA will interfere with ribosome recruitment. To further explore this possibility, we performed a toe-print experiment. The results from a toe-print analysis of *oppA* RNA in the absence or presence of Rli22 is presented in Fig. 10A. In the absence of the sRNA, a strong RT pause was observed at +16 (relative to the translational start site), signifying specific binding of the *E. coli* 30S ribosome to the *oppA* RNA. Upon addition of wild type Rli22, this band was diminished, demonstrating that Rli22 binding efficiently prevents the formation of a ribosomal complex. To evaluate whether either of the CU-rich regions were able to prevent ribosome binding on its own, toe-print analysis of *oppA* RNA incubated with Rli22_mut_loopA or Rli22_mut_ss was carried out (Fig. 10A). For both mutant variants, ribosome binding was efficiently inhibited, albeit to a lesser extent than for wild type Rli22. Finally, when *oppA* RNA was incubated with the Rli22 double mutant, the toe-print at +16 was re-established. Thus, mutation of both UCCC motifs in Rli22 disrupts the inhibitory function of the sRNA on the formation of the ribosomal complex. In the case of Rli33-1 (Fig. 10B), no toe-print was observed in the presence of wild type Rli33-1, corresponding to an inhibition of ribosome binding to *oppA* mRNA. When incubated with the single mutants of Rli33-1, the toe-print was diminished to a lesser extent than for wild type Rli33-1. Furthermore, slight differences between the 2 single mutants were observed: compared to Rli33-1_mut_ss, higher concentrations of Rli33-1_mut_loopA were required to prevent formation of the ribosomal complex. Finally, when both UCCC motifs of Rli33-1 were disrupted a strong toe-print was formed, showing that this mutant variant was unable to prevent ribosome binding.

Taken together, the toe-print analyses demonstrated that both Rli22 and Rli33-1 are able to prevent the ribosome from binding to the SD region of *oppA* mRNA, and that this inhibitory effect is exerted through the UCCC motifs of the sRNAs. The inhibitory activity of the mutant sRNAs correlates with their individual *oppA* binding affinities. Thus, efficient binding of a CU-rich region to the SD region of *oppA* mRNA blocks formation of the ribosomal complex.

Discussion

In recent years, bacterial multicopy sRNAs have received increasing attention. Given their sequence similarity, it might be expected that multicopy sRNAs control the expression of the same set of target genes, thus performing redundant regulatory functions. However, homologous sRNAs might also act non-redundantly, as a result of differential regulation of the genes encoding the individual sRNAs.[36,37] Alternatively, non-redundant activities may arise if highly homologous sRNAs act by different molecular mechanisms, and/or if individual sRNAs control the expression of unique sets of target genes relative to their siblings.[38,39]

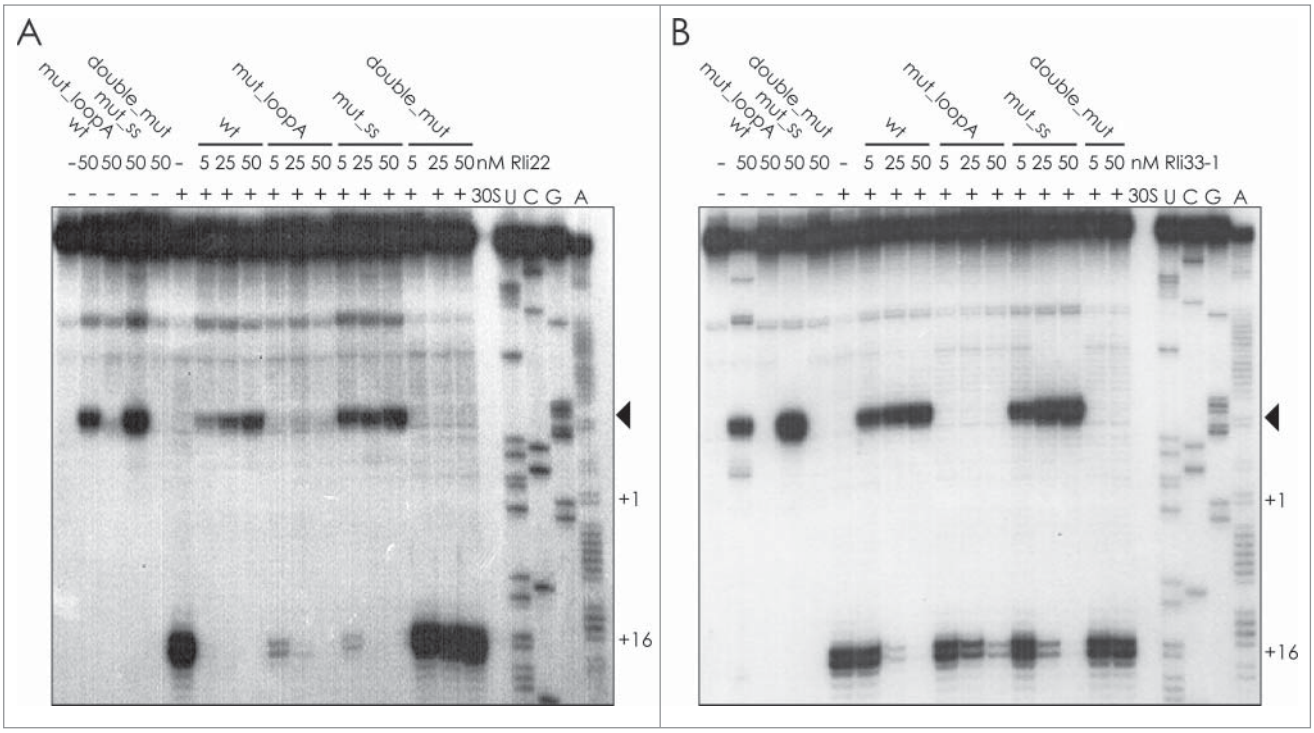

Figure 10. Rli22 and Rli33-1 inhibit the formation of the translation initiation complex on *oppA* mRNA. The ability of the sRNAs to inhibit the formation of the translation initiation complex on *oppA* mRNA was investigated by toe-print assay. The *oppA* RNA was incubated with increasing concentrations of either wild type Rli22 and its mutant variants (A), or wild type Rli33-1 and its mutants variants (B) to reach molar ratios of 1:1. The samples were subjected to reverse transcription in the prescence of *E. coli* 30S ribosome and $tRNA^{met}$. RT pauses caused by strong sRNA binding are signified by a black arrow. The position of the toeprint (+16) and the translational start site (+1) are indicated. The experiment was repeated 3 times with similar results.

In this study, we show that the homologous sRNAs Rli22 and Rli33-1 are structurally and functionally related to the multicopy sRNA LhrC, acting to down-regulate expression of the virulence adhesin LapB, the oligo-peptide binding protein OppA, and the $CD4^+$ T cell-stimulating antigen TcsA.[23,24] Interestingly, these cell envelope-associated proteins are required for full virulence of *L. monocytogenes*.[25,27, 28] Likewise, LhrC1-5 and Rli33-1 have been shown to contribute to listerial infection.[12,24] In order to avoid detection by immune cells during infection, a strict regulation of surface exposed proteins is pivotal. Since LhrC1-5, Rli22 and Rli33-1 are all induced during infection-related conditions (Table 1), it is possible that the main role of this family of sRNAs is to modulate the expression of cell envelope-associated proteins otherwise recognized by the host immune system. Like LhrC1-5, Rli22 and Rli33-1 negatively regulate expression of *lapB, oppA* and *tcsA* at the post-transcriptional level, suggesting that these homologous sRNAs may act in a redundant manner. Indeed, *in vitro* binding studies of individual sRNAs showed that they interact with the SD region in the *oppA* mRNA, similar to their sibling sRNAs (illustrated in Fig. 11A). Rli22 and Rli33-1 each hold 2 CU-rich regions also shared by the 5 LhrCs. The CU-rich regions are characterized by a highly conserved UCCC motif, which is essential for sRNA-mRNA interactions, flanked by less conserved sequences that also contribute to target recognition. We have previously shown that the UCCC motifs residing within the single-stranded stretch and the terminator loop of LhrC4 are important for binding to the SD region of the *oppA* mRNA, whereas the UCCC motif in loop A is dispensable for LhrC4-*oppA* mRNA interaction.[24] Intriguingly, the 2 CU-rich regions in LhrC4 involved in binding *oppA* mRNAs are homologous to the 2 CU-rich regions in Rli22 and Rli33-1 (Fig. 1A), suggesting that the sRNAs might share similar target mRNAs. Indeed, we found that the 2 CU-rich regions of Rli22/Rli33-1 are capable of binding the SD region of *oppA* mRNA, albeit with slightly different affinities. Just one of the UCCC motifs is sufficient for preventing the formation of a ribosomal complex *in vitro*. The *in vitro* and *in vivo* data suggested that the primary effect of these sRNAs is to prevent the recruitment of the ribosome at the initiation step subsequently followed by mRNA degradation. Thus, the redundant regulatory activity of LhrC1-5, Rli22 and Rli33-1 on *oppA* correlates well with the presence of highly conserved CU-rich regions in each of the 7 sRNAs (Fig. 11A). This sRNA family poses the first example of sRNAs containing multiple binding sites for the same region of an mRNA. CU-rich motifs have been shown to be a common feature of sRNAs in Gram-positive species.[19,29-32] However, while these motifs have been shown to be important for mRNA interaction *in vitro*, so far their relevance *in vivo* has rarely been addressed.[40,41] In this study we provide evidence that the UCCC motifs are involved in the post-transcriptional regulation of target genes, and that disruption of both regions in Rli22 or Rli33-1 abolishes sRNA-mediated regulation *in vivo* (Fig. 2 and 3).

The addition of Rli22 and Rli33-1 to the family of LhrC sRNAs brings this family up to a total of 7 members in *L. monocytogenes* LO28 and, for other *L. monocytogenes* strains, a copy number between 5 and 7 is observed.[42] Thus, the LhrC family contains the highest number of sibling sRNAs reported so far in a single bacterium. sRNA multiplicity has been observed in a variety of bacterial species, as exemplified by 4-5 copies of Qrr sRNAs in *Vibrio* species[21,22] and up to 6 copies of csRNA in *Streptococcus* species.[19,20] Intriguingly, the LhrC1-5, Rli22 and Rli33-1 sRNAs confer an additional layer of multiplicity, since each individual sRNA holds 2 or 3 CU-rich mRNA-binding sites. Single-copy sRNAs in Gram-positive bacteria, such as RNAIII in *S. aureus* and FasX of *Streptococcus pyrogenes*, hold more than one CU-rich motif as well. However, in the case of RNAIII, the individual motifs bind to distant regions of the same target mRNA encoded by *coa*,[31] whereas FasX uses its 2 CU-rich regions for binding of 2 different target mRNAs, encoded by *ska* and *cpa*, respectively.[30] Thus, the multiple binding sites of LhrC1-5, Rli22 and Rli33-1, targeting the same region of *oppA* mRNA, poses a unique example of multiplicity, allowing simultaneous binding of 2 *oppA* mRNAs to each sRNA (Fig. 11A). However, it also raises an interesting question: Why do 7 highly homologous sRNAs target the same mRNA? The regulatory effect exerted by a single sRNA appears to be relatively subtle (Fig. 2 and 3). Thus, when expressed individually, these sRNAs seem to act as fine-tuners. However, when produced simultaneously, they may allow for a much stronger regulation of their mutual target genes.[23,24]

Despite their structural and functional similarity, some differences were noted between LhrC1-5, Rli22 and Rli33-1 (Table 1; Fig. 11B). More specifically, the expression of Rli33-1 relies on the general stress sigma factor σ^B, whereas induction of Rli22 and LhrC1-5 in response to cell envelope stress depends on the TCS LisRK. In line with this, Rli33-1 is uniquely induced in the stationary growth phase,[14] suggesting that Rli33-1 might perform unique functions in the bacterium under this condition. In response to cefuroxime exposure, Rli22 and LhrC1-5 are expressed, suggesting that these 6 LisRK-regulated sRNAs might hold overlapping regulatory functions in response to cell envelope stress. Furthermore, different levels of Rli22 in a wild type strain vs. a strain lacking LhrC1-5 expression might imply a regulatory interconnection between these sRNAs. However, when residing in the intestinal lumen of mice, Rli22 is uniquely induced, whereas the level of LhrC1-5 and Rli33-1 remains unaffected, indicating that Rli22 performs regulatory functions independently of LhrC1-5 and Rli33-1 in the intestinal phase of infection.[14] Finally, we note that under some conditions, such as exposure to whole human blood, all 7 sRNAs are induced, indicating that the regulatory activity of each and every one of them might be required when *Listeria* reaches the bloodstream.[14] Thus, although LhrC1-5, Rli22 and Rli33-1 are structurally and functionally related, they are also differentially expressed, suggesting that they might perform independent activities in the bacterium under the conditions where they are uniquely produced.

With respect to *tcsA*, the sRNAs appear to employ different mechanisms to regulate this target gene. Clearly, the individual sRNAs hold the capacity of down-regulating the expression of *tcsA in vivo* (Fig. 2 and 3) but *in vitro* binding studies revealed that only the LhrC homolog was capable of base pairing to tcsA mRNA (Fig. S7). Although they were predicted to bind to the SD region, neither Rli22 nor Rli33-1 were able to interact with *tcsA* mRNA *in vitro*, further suggesting that the 7 sRNAs, though similar in sequence and function, are capable of employing different mechanisms of regulation. The distinct

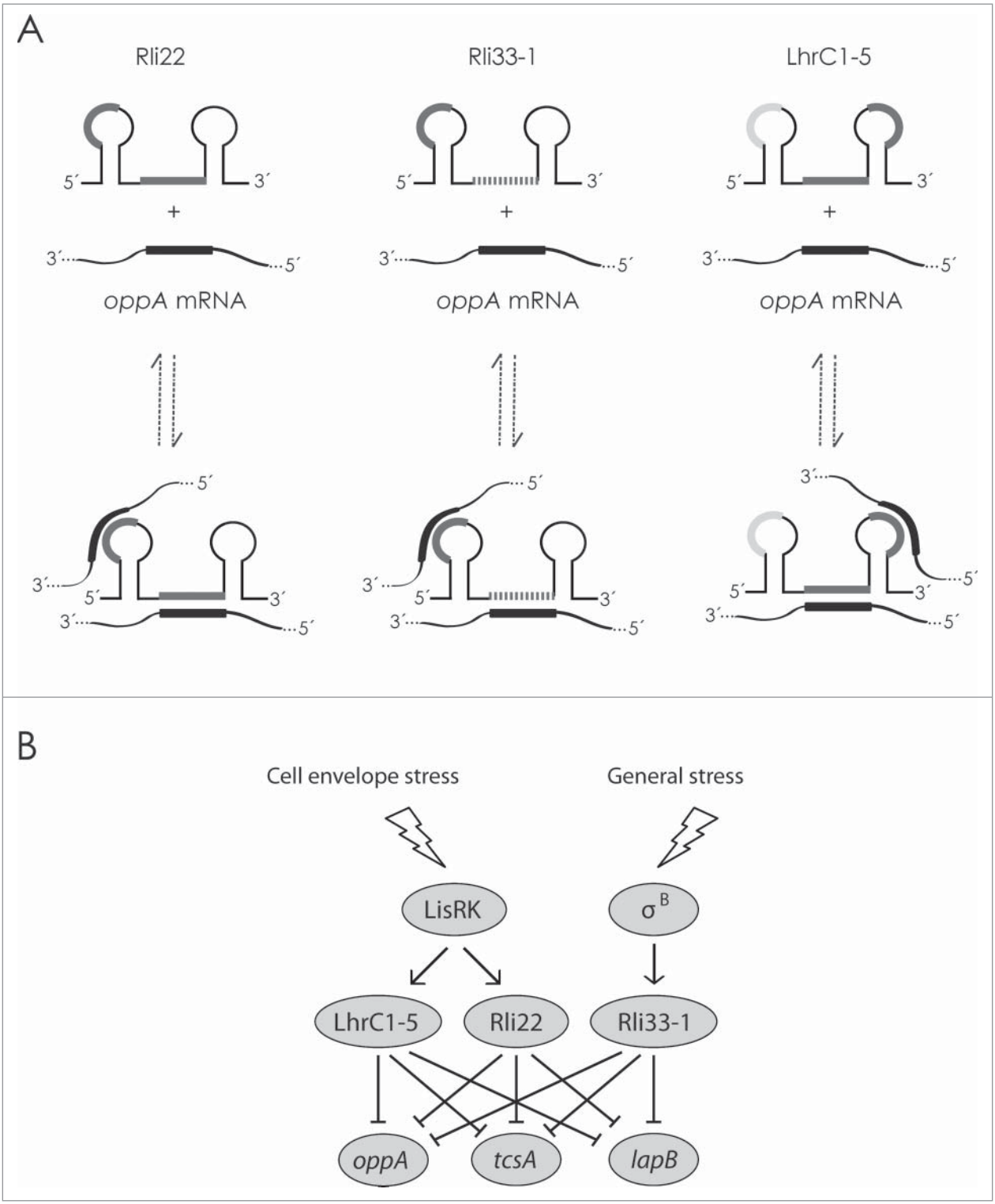

Figure 11. The shared and distinctive characteristics of the LhrC family. (A) Model demonstrating the similar *oppA* mRNA binding mechanisms exerted by Rli22, Rli33-1 and LhrC1-5. Each sRNA is capable of binding the SD region of *oppA* mRNA through 2 conserved UCCC motifs. The mRNA binding sites of the sRNAs are either indicated in dark gray, if the interaction with *oppA* mRNA is strong, or shaded gray, if the interaction is weak. The binding region in *oppA* mRNA is marked in black. For Rli22 and Rli33-1, the UCCC motif of the loop A region as well as the single-stranded stretch are able to bind *oppA* mRNA, however, for Rli33-1, the loop A region is the preferred binding site. LhrC1-5 binds *oppA* mRNA through the UCCC motifs in the single-stranded region and the terminator loop; the additional UCCC motif in loop A (light gray) does not contribute to *oppA* RNA interaction. (B) Model illustrating the differential expression of the sRNAs. While LhrC1-5 and Rli22 are induced in response to cell envelope stress by the two-component system LisRK, expression of Rli33-1 is induced by the general stress factor σ^B. All of the sRNAs are able to down-regulate the expression of *oppA, tcsA* and *lapB* at the post-transcriptional level.

mechanisms underlying the *in vivo* regulation of *tcsA* by each sRNA remain to be elucidated. However, the results obtained so far indicate that regulation of *tcsA* by Rli22 or Rli33-1 might depend on the assistance of co-factors. For Gram-negative species, sRNA-mediated regulation generally involves the RNA chaperone Hfq.[1,2] Surprisingly, though present in many

Gram-positive bacteria, the contribution of Hfq to sRNA-mediated control in these bacterial species remains elusive.[43,44] At present, the sRNA LhrA in *L. monocytogenes* poses the only example of a Gram-positive sRNA dependent on Hfq.[45,46] With respect to LhrC, this multicopy sRNA was initially identified as an Hfq-binding sRNA.[15] The LhrC sRNAs interact with Hfq *in vivo* and *in vitro*; however, a function for Hfq in LhrC-mediated control remains to be shown. In the present study, we observed that Rli22 and Rli33-1 do not bind Hfq *in vitro*, further setting apart these 2 sRNAs from the Hfq-binding LhrCs. A recent study shows that *Listerial* Hfq has a very weak annealing activity and does not recognize A-rich target RNAs in contrast to *E. coli* Hfq.[47] The unessential role of Hfq in many Gram-positive bacteria raises the question of whether other protein factors facilitate sRNA-mediated regulation in these bacterial species. Thus, it could be speculated that the *in vivo* regulation exerted by Rli22 and Rli33-1 on *tcsA* rely on such an unidentified co-factor.

When comparing the 5 LhrCs, it is clear that they exhibit a high degree of sequence identity (>85 %). Rli22 and Rli33-1 are 64% identical at the nucleotide level. Furthermore, LhrC1-5 share from 55% to 60% identity with Rli22 and Rli33-1, with the majority of sequence similarity spanning the conserved CU-rich regions (Fig. 1B). The UCCC motifs provide the seed sequence to directly target mRNAs with a strong SD-sequence,[32,48] which could explain the pressure of selection for maintaining these regions. Although the CU-rich regions of the sRNAs are highly similar in sequence, their flanking regions are less conserved (Fig. 1B), which may allow the sibling sRNAs to have unique targets as well. Examples of homologous sRNAs sharing overlapping as well as exclusive functions have been reported.[49] The multicopy sRNA Qrr of *Vibro* species hold several binding sites able to interact with different target mRNAs. Interestingly, the Qrr1 sRNA lacks one of the critical pairing regions for target recognition, leading to a less effective regulation of a subset of target genes.[39,50] Otherwise, Qrr1 is as functional as its siblings in controlling other Qrr target genes through the sequences conserved in all Qrr sRNAs. In the present study, Rli22 and Rli33-1 were investigated in the context of LhrC1-5 target genes. Thus, unique targets of Rli22 and Rli33-1 are yet to be identified. In future studies it will be interesting to determine and compare the regulons for each of the 7 sRNAs. In light of the findings reported so far, we would expect to see individual targets as well as genes regulated by all 7 sRNAs.

All together, these 7 sRNAs hold an impressive number of 19 CU-rich sites for specific recognition of target mRNAs, rendering this family a unique case of multiplicity and complexity. Unraveling the shared and unique functions of the sRNAs and their regulatory regions is needed in order to better understand why *L. monocytogenes* possesses multiple copies of the same sRNA. Multicopy sRNAs are often regulators of essential cellular processes, such as iron homeostasis, quorum sensing and virulence, in which a precise regulation is pivotal.[51,52] LhrC1-5 and Rli33-1 have been shown to be involved in listerial pathogenicity[12,24] and all 7 sRNAs are expressed under various infection-relevant conditions.[12,14,23] In the present study, we furthermore demonstrated that 3 genes encoding the virulence-associated proteins OppA, TcsA and LapB are down-regulated by all the members of this family of highly related sRNAs. Collectively, these 7 homologous sRNAs represent a fascinating case for future studies on the purpose of sRNA multiplicity in the context of bacterial virulence.

Experimental procedures

Bacterial strains and growth conditions

The wild type strains used in this study were *L. monocytogenes* serotype 1/2c LO28[53] and EGD serotype 1/2a EGD-e (obtained from W. Goebel, University of Wurzburg, Wurzburg, Germany). The isogenic mutant derivatives LO28Δ*lhrC1-5*,[23] LO28Δ*lisR*,[54] and EGDΔ*sigB*[55] were constructed in previous work. An LO28 strain lacking chromosomal expression of all 7 sRNAs (LO28-Δ7) was constructed for this study by subsequent in-frame deletion of *rli22* and *rli33-1* in LO28Δ*lhrC1-5*. This strain was used for construction of strains with chromosomal expression of sRNAs from the *lhrC5* promoter. *L. monocytogenes* was routinely grown at 37°C with aeration in brain heart infusion broth (BHI, Oxoid) unless stated otherwise. When appropriate, cultures were supplemented with kanamycin (50 μg/ml) or erythromycin (5 μg/ml). For induction of sRNA expression, cultures were supplemented with cefuroxime (4 μg/ml) or NaCl (3.5%). For cloning of plasmid vectors, *Escherichia coli* TOP10 cells (Invitrogen) were grown at 37°C with aeration in Luria-Bertani broth supplemented with kanamycin (50 μg/ml) or erythromycin (150 μg/ml), when appropriate.

Construction of LO28-Δ7 and mutant derivatives

For chromosomal in-frame insertion and deletion in *L. monocytogenes*, the temperature-sensitive shuttle vector pAUL-A was used.[56] All fragments were amplified from chromosomal DNA in a 2-step PCR procedure (primers are listed in Table S1). For deletion of *rli22* and *rli33-1*, fragments consisting of the flanking region of the gene were constructed. For insertions downstream of the *lhrC5* promoter, the PCR fragments consisted of the flanking regions of *lhrC5* and the coding sequence of either *rli22, rli33-1* or mutant derivatives thereof. All fragments were digested with EcoRI and BamHI before ligation into pAUL-A; the resulting plasmids were introduced into *L. monocytogenes* by electroporation.[57] Homologous recombination was achieved as previously described.[58]

Plasmid constructions and β-galactosidase assays

To examine the transcriptional activity of *rli22* and *rli33-1*, we used the promoter-less *lacZ* transcriptional fusion vector pTCV-lac.[59] The promoter region of *rli22* and *rli33-1* was acquired by PCR from chromosomal DNA, digested with EcoRI and BamHI (primers are listed in Table S1), and ligated into pTCV-lac.

Post-transcriptional regulation of LhrC target genes was monitored using in-frame translational *lacZ* fusions of *oppA, tcsA* and *lapB* constructed in previous work.[23,24] Briefly, DNA fragments encoding a moderate core promoter[45] as well as a region spanning the SD region of either *oppA* (−41 to +32),

tcsA (−133 to +53), or *lapB* (−100 to +32) were ligated into pCK-lac.[46]

Cells were harvested for β-galactosidase assays as described previously.[58] Briefly, cultures were grown to OD_{600}= 0.2 (for strains with translational fusions) or OD_{600} = 0.35 (for strains with transcriptional fusions). Cultures were then split and one half stressed as described above. Samples (1 ml) were withdrawn prior to stress and at indicated time points after the onset of stress. β-galactosidase assays were conducted as described in[60] and results were analyzed using two-tailed ANOVA. The differences reported were statistically significant with at least 95% confidence.

RNA isolation and purification

For primer extension and northern blot analysis, *L. monocytogenes* was grown to OD_{600} = 0.35 (unless stated otherwise). Cultures were then split and one half stressed. Samples were taken from stressed and control cultures after 1 and 2 hours. Cells were harvested by centrifugation for 5 min at 5000 xg at 4°C and snap-frozen in liquid nitrogen. Cells were disrupted by the FastPrep instrument (Bio101, Thermo Scientific Corporation) and total RNA was extracted using TRIzol® Reagent (Ambion®) as previously described.[46] The integrity, concentration and purity of the RNA were confirmed by agarose gel electrophoresis and NanoDrop 2000.

Primer extension

Primer extension experiments were performed as previously described.[58] The ^{32}P-labeled, single-stranded primers used for detection of *rli22* and *rli33-1* transcription start sites are listed in Table S1.

Northern blotting

Total RNA (10 μg) was resolved on a 6% polyacrylamide-8 M urea gel as previously described. ref 36; *oppA* and *tcsA* mRNAs were detected by RNA gel blotting as described previously.[24] Membranes were hybridized as described in[58] using the ^{32}P-labeled, single-stranded probes listed in Table S1. RNA bands were visualized using a Typhoon Trio (GE Healthcare) and analyzed with IQTL 8.0 quantification software (GE Healthcare).

In silico *prediction of sRNA-mRNA interaction and RNA secondary structure predictions*

The IntaRNA software[34,35] was used for predicting interactions between target mRNAs and sRNAs. Full length sequences of sRNAs and targets were employed. Secondary structure predictions were obtained by use of Mfold.[61]

Electrophoretic mobility shift assays (EMSA)

Templates for *in vitro* transcription carried a T7 RNA polymerase binding site at their 5′-end and were generated by PCR. Templates for *tcsA, oppA*, and *lapB* were obtained by PCR from chromosomal DNA and templates for *oppA*_mut and sRNA transcripts were made using overlapping primers. The primers are listed in Table S1. *In vitro* transcription, RNA purification, dephosphorylation and labeling were performed as described previously.[23] EMSAs were performed as previously described.[46] Briefly, 40 fmol of 5′-end labeled RNA was incubated with excess unlabeled RNA or purified Hfq protein[15] to a total volume of 10 μl in the presence of non-specific competitor (tRNA) for 1 hour at 37°C followed by 10 min on ice. For the EMSA of sRNAs and *tcsA*, Rli22 or Rli33-1 were incubated with *tcsA* RNA, heated to 70°C and slow cooled to 37°C, prior to incubation for 1 hour at 37°C. All samples were separated on a 5% non-denaturing gel at 4°C. RNA bands were visualized and quantified as described for northern blotting experiments.

In vitro *enzymatic probing*

T7-transcribed *oppA* and sRNA variants were dephosphorylated using Fast AP alkaline phosphatase (Fermentas) according to manufacturer's guidelines. RNA was purified by phenol-chloroform extraction as previously described.[62] RNA was 5′-end labeled using [$\gamma-^{32}$P] and T4 polynucleotide kinase (Ambion) according to manufacturer's guidelines and subsequently purified on a 6% polyacrylamide-8 M urea gel. The enzymatic probing was carried out as described previously,[62] with some deviations. Briefly, labeled RNA (50,000 cps) was denatured at 90°C for 1 min and cooled on ice for 1 min, after which the RNA was incubated at 20°C for 15 min in the presence of 10 mM $MgCl_2$ and monovalent ions (KCl) to allow for renaturation. For structural probing with *oppA*, various concentrations of cold renatured *oppA* were added and samples were incubated for an additional 15 min. Samples were treated with the indicated cleaving agents: 0.004 U V1 RNase (Ambion) for 5 min, 0.5 U of T1 RNase (Thermo scientific) for 5 min, and 0.025 U T2 RNase (MoBiTech) for 10 min. All reactions were performed at 20°C and were terminated by adding 190 μl 0.3 M NaAc followed by phenol chloroform extraction and precipitation with ethanol. The RNase T1 ladder and alkaline ladder were made according to a protocol previously described.[62] Samples were separated on a 12% polyacrylamide-8 M urea gel.

DMS alkylation

Five pmol *oppA* transcript was denatured as described for enzymatic probing and renatured at 20°C for 15 min in 50 mM HEPES (pH 7.5), 5 mM $MgCl_2$ and 75 mM KCl. sRNA transcripts were added in various concentrations and samples were incubated at 20°C for an additional 15 min, after which samples were supplemented with 1 μg of tRNA and treated with 1.3 M DMS (Acros) for 5 min. The reaction was terminated by RNA precipitation in 1 M Guanidine thiocyanate (Sigma), 0.167% N-Lauryl sarcosine (Sigma), 10 mM DTT, and 83% isopropanol. Next, DMS-modified *oppA* was hybridized with ^{32}P-labeled oligo *oppA*_165_nt_rev (Table S1) (50,000 cps) by successive incubation: 2 min at 90°C and 1 min on ice followed by incubation of 5 min at 20°C in RT buffer (QBIOgene). Reverse transcription was carried out at 37°C for 30 min in RT buffer in the presence of 0.33 mM dNTP and 2 U AMV-RT (Life Sciences). For the sequencing reaction, the reverse transcription

was performed on unmodified *oppA* transcript in the presence of ddNTP. After primer extension, RNA templates were degraded by adding KOH (3 M) in a buffer containing 50 mM Tris-HCl (pH 8.0), 0.5% SDS and 7.5 mM EDTA at 90°C for 3 min, followed by incubation at 37°C for 1 hour. DNA was precipitated with ethanol and samples were run on a 10% polyacrylamide-8 M urea gel.

Toe-printing

E. coli 30S ribosome was purified and the toe-printing assay was performed as described previously with a few deviations.[63] Briefly, *oppA* transcript (50 nM) together with ^{32}P-labeled oligo *oppA*_165_nt_rev (50,000 cps; Table S1) were hybridized as described for DMS alkylation and the mRNA was then incubated for 15 min at 20°C in the presence of $MgCl_2$ and monovalent ions (KCl). In parallel, 30S ribosomal subunits were preincubated at 37°C for 10 min. Ribosomal subunit (50 nM), renatured sRNA transcripts, and $MgCl_2$ (to a final concentration of 8.5 mM) were then added and samples were incubated at 37°C for 15 min. Finally, $tRNA^{fMet}$ was added and the incubation was continued for 5 min. Reverse transcription was performed by addition of AMV-RT (2 U per reaction) and dNTPs (0.33 mM) followed by incubation at 37°C for 30 min. Reactions were stopped by phenol-chloroform extraction and subsequent precipitation with ethanol, and samples were loaded onto a 10% polyacrylamide-8 M urea gel.

Disclosure of potential conflicts of interest

No potential conflicts of interest were disclosed.

Acknowledgment

We thank Stefano Marzi for excellent advice on the toe-printing assays.

Funding

This work was supported by The Danish Council for Independent Research | Natural Sciences [12–124735 to B.H.K.]; VILLUM FONDEN to [B.H.K.]; The Lundbeck Foundation to [B.H.K.] and Novo Nordisk Foundation to [B.H.K]. This work was also supported by the Center National de la Recherche Scientifique (CNRS) to [P.R.] and has been published under the framework of the LABEX: ANR-10-LABX-0036 NETRNA to [P.R.], a funding from the state managed by the French National Research Agency as part of the investments for the future program.

References

1. Storz G, Vogel J, Wassarman KM. Regulation by small RNAs in bacteria: expanding frontiers. Mol Cell 2011; 43:880-91; PMID:21925377; http://dx.doi.org/10.1016/j.molcel.2011.08.022
2. Waters LS, Storz G. Regulatory RNAs in bacteria. Cell 2009; 136:615-28; PMID:19239884; http://dx.doi.org/10.1016/j.cell.2009.01.043
3. Gripenland J, Netterling S, Loh E, Tiensuu T, Toledo-Arana A, Johansson J. RNAs: regulators of bacterial virulence. Nat Rev Microbiol 2010; 8:857-66; PMID:21079634; http://dx.doi.org/10.1038/nrmicro2457
4. Papenfort K, Vogel J. Small RNA functions in carbon metabolism and virulence of enteric pathogens. Front Cell Infect Microbiol 2014; 4:91; PMID:25077072; http://dx.doi.org/10.3389/fcimb.2014.00091
5. Ortega AD, Quereda JJ, Pucciarelli MG, Garcia-del Portillo F. Non-coding RNA regulation in pathogenic bacteria located inside eukaryotic cells. Front Cell Infect Microbiol 2014; 4:162; PMID:25429360; http://dx.doi.org/10.3389/fcimb.2014.00162
6. Mellin JR, Cossart P. The non-coding RNA world of the bacterial pathogen *Listeria monocytogenes*. RNA Biol 2012; 9:372-8; PMID:22336762; http://dx.doi.org/10.4161/rna.19235
7. Allerberger F, Wagner M. Listeriosis: a resurgent foodborne infection. Clin Microbiol Infect 2010; 16:16-23; PMID:20002687; http://dx.doi.org/10.1111/j.1469-0691.2009.03109.x
8. Swaminathan B, Gerner-Smidt P. The epidemiology of human listeriosis. Microbes Infect 2007; 9:1236-43; PMID:17720602; http://dx.doi.org/10.1016/j.micinf.2007.05.011
9. Nielsen JS, Olsen AS, Bonde M, Valentin-Hansen P, Kallipolitis BH. Identification of a sigma B-dependent small noncoding RNA in *Listeria monocytogenes*. J Bacteriol 2008; 190:6264-70; PMID:18621897; http://dx.doi.org/10.1128/JB.00740-08
10. Mandin P, Repoila F, Vergassola M, Geissmann T, Cossart P. Identification of new noncoding RNAs in *Listeria monocytogenes* and prediction of mRNA targets. Nucleic Acids Res 2007; 35:962-74; PMID:17259222; http://dx.doi.org/10.1093/nar/gkl1096
11. Behrens S, Widder S, Mannala GK, Qing X, Madhugiri R, Kefer N, Abu Mraheil M, Rattei T, Hain T. Ultra deep sequencing of *Listeria monocytogenes* sRNA transcriptome revealed new antisense RNAs. PLoS One 2014; 9:e83979; PMID:24498259; http://dx.doi.org/10.1371/journal.pone.0083979
12. Mraheil MA, Billion A, Mohamed W, Mukherjee K, Kuenne C, Pischimarov J, Krawitz C, Retey J, Hartsch T, Chakraborty T, et al. The intracellular sRNA transcriptome of *Listeria monocytogenes* during growth in macrophages. Nucleic Acids Res 2011; 39:4235-48; PMID:21278422; http://dx.doi.org/10.1093/nar/gkr033
13. Oliver HF, Orsi RH, Ponnala L, Keich U, Wang W, Sun Q, Cartinhour SW, Filiatrault MJ, Wiedmann M, Boor KJ. Deep RNA sequencing of *L. monocytogenes* reveals overlapping and extensive stationary phase and sigma B-dependent transcriptomes, including multiple highly transcribed noncoding RNAs. BMC Genomics 2009; 10:641; PMID:20042087; http://dx.doi.org/10.1186/1471-2164-10-641
14. Toledo-Arana A, Dussurget O, Nikitas G, Sesto N, Guet-Revillet H, Balestrino D, Loh E, Gripenland J, Tiensuu T, Vaitkevicius K, et al. The Listeria transcriptional landscape from saprophytism to virulence. Nature 2009; 459:950-6; PMID:19448609; http://dx.doi.org/10.1038/nature08080
15. Christiansen JK, Nielsen JS, Ebersbach T, Valentin-Hansen P, Sogaard-Andersen L, Kallipolitis BH. Identification of small Hfq-binding RNAs in *Listeria monocytogenes*. RNA 2006; 12:1383-96; PMID:16682563; http://dx.doi.org/10.1261/rna.49706
16. Mellin JR, Koutero M, Dar D, Nahori MA, Sorek R, Cossart P. Riboswitches. Sequestration of a two-component response regulator by a riboswitch-regulated noncoding RNA. Science 2014; 345:940-3; PMID:25146292; http://dx.doi.org/10.1126/science.1255083
17. Peng YL, Meng QL, Qiao J, Xie K, Chen C, Liu TL, Hu ZX, Ma Y, Cai XP, Chen CF. The roles of noncoding RNA Rli60 in regulating the virulence of *Listeria monocytogenes*. J Microbiol Immunol Infect 2014; S1684-1182(14)00186-8
18. Torres-Quesada O, Millan V, Nisa-Martinez R, Bardou F, Crespi M, Toro N, Jimenez-Zurdo JI. Independent activity of the homologous small regulatory RNAs AbcR1 and AbcR2 in the legume symbiont *Sinorhizobium meliloti*. PLoS One 2013; 8:e68147; PMID:23869210; http://dx.doi.org/10.1371/journal.pone.0068147
19. Halfmann A, Kovacs M, Hakenbeck R, Bruckner R. Identification of the genes directly controlled by the response regulator CiaR in *Streptococcus pneumoniae*: five out of 15 promoters drive expression of small non-coding RNAs. Mol Microbiol 2007; 66:110-26; PMID:17725562; http://dx.doi.org/10.1111/j.1365-2958.2007.05900.x
20. Marx P, Nuhn M, Kovacs M, Hakenbeck R, Bruckner R. Identification of genes for small non-coding RNAs that belong to the regulon of the two-component regulatory system CiaRH in *Streptococcus*. BMC Genomics 2010; 11:661; PMID:21106082; http://dx.doi.org/10.1186/1471-2164-11-661
21. Tu KC, Bassler BL. Multiple small RNAs act additively to integrate sensory information and control quorum sensing in *Vibrio harveyi*.

Genes Dev 2007; 21:221-33; PMID:17234887; http://dx.doi.org/10.1101/gad.1502407
22. Lenz DH, Mok KC, Lilley BN, Kulkarni RV, Wingreen NS, Bassler BL. The small RNA chaperone Hfq and multiple small RNAs control quorum sensing in Vibrio harveyi and Vibrio cholerae. Cell 2004; 118: 69-82; PMID:15242645; http://dx.doi.org/10.1016/j.cell.2004.06.009
23. Sievers S, Sternkopf Lillebaek EM, Jacobsen K, Lund A, Mollerup MS, Nielsen PK, Kallipolitis BH. A multicopy sRNA of *Listeria monocytogenes* regulates expression of the virulence adhesin LapB. Nucleic Acids Res 2014; 42:9383-98; PMID:25034691; http://dx.doi.org/10.1093/nar/gku630
24. Sievers S, Lund A, Menendez-Gil P, Nielsen A, Storm Mollerup M, Lambert Nielsen S, Buch Larsson P, Borch-Jensen J, Johansson J, Kallipolitis BH. The multicopy sRNA LhrC controls expression of the oligopeptide-binding protein OppA in *Listeria monocytogenes*. RNA Biol 2015; 12:985-97; PMID:26176322; http://dx.doi.org/10.1080/15476286.2015.1071011
25. Reis O, Sousa S, Camejo A, Villiers V, Gouin E, Cossart P, Cabanes D. LapB, a novel *Listeria monocytogenes* LPXTG surface adhesin, required for entry into eukaryotic cells and virulence. J Infect Dis 2010; 202:551-62; PMID:20617901; http://dx.doi.org/10.1086/654880
26. Sanderson S, Campbell DJ, Shastri N. Identification of a CD4+ T cell-stimulating antigen of pathogenic bacteria by expression cloning. J Exp Med 1995; 182:1751-7; PMID:7500019; http://dx.doi.org/10.1084/jem.182.6.1751
27. Borezee E, Pellegrini E, Berche P. OppA of *Listeria monocytogenes*, an oligopeptide-binding protein required for bacterial growth at low temperature and involved in intracellular survival. Infect Immun 2000; 68:7069-77; PMID:11083832; http://dx.doi.org/10.1128/IAI.68.12.7069-7077.2000
28. Port GC, Freitag NE. Identification of novel *Listeria monocytogenes* secreted virulence factors following mutational activation of the central virulence regulator, PrfA. Infect Immun 2007; 75:5886-97; PMID:17938228; http://dx.doi.org/10.1128/IAI.00845-07
29. Patenge N, Pappesch R, Khani A, Kreikemeyer B. Genome-wide analyses of small non-coding RNAs in *streptococci*. Front Genet 2015; 6:189; PMID:26042151; http://dx.doi.org/10.3389/fgene.2015.00189
30. Miller EW, Cao TN, Pflughoeft KJ, Sumby P. RNA-mediated regulation in Gram-positive pathogens: an overview punctuated with examples from the group A *Streptococcus*. Mol Microbiol 2014; 94:9-20; PMID:25091277; http://dx.doi.org/10.1111/mmi.12742
31. Chevalier C, Boisset S, Romilly C, Masquida B, Fechter P, Geissmann T, Vandenesch F, Romby P. *Staphylococcus aureus* RNAIII binds to two distant regions of *coa* mRNA to arrest translation and promote mRNA degradation. PLoS Pathog 2010; 6:e1000809; PMID:20300607; http://dx.doi.org/10.1371/journal.ppat.1000809
32. Geissmann T, Chevalier C, Cros MJ, Boisset S, Fechter P, Noirot C, Schrenzel J, Francois P, Vandenesch F, Gaspin C, et al. A search for small noncoding RNAs in *Staphylococcus aureus* reveals a conserved sequence motif for regulation. Nucleic Acids Res 2009; 37:7239-57; PMID:19786493; http://dx.doi.org/10.1093/nar/gkp668
33. Pischimarov J, Kuenne C, Billion A, Hemberger J, Cemic F, Chakraborty T, Hain T. sRNAdb: a small non-coding RNA database for gram-positive bacteria. BMC Genomics 2012; 13:384; PMID:22883983; http://dx.doi.org/10.1186/1471-2164-13-384
34. Busch A, Richter AS, Backofen R. IntaRNA: efficient prediction of bacterial sRNA targets incorporating target site accessibility and seed regions. Bioinformatics 2008; 24:2849-56; PMID:18940824; http://dx.doi.org/10.1093/bioinformatics/btn544
35. Wright PR, Georg J, Mann M, Sorescu DA, Richter AS, Lott S, Kleinkauf R, Hess WR, Backofen R. CopraRNA and IntaRNA: predicting small RNA targets, networks and interaction domains. Nucleic Acids Res 2014; 42: W119-23; PMID:24838564; http://dx.doi.org/10.1093/nar/gku359
36. Deng Z, Meng X, Su S, Liu Z, Ji X, Zhang Y, Zhao X, Wang X, Yang R, Han Y. Two sRNA RyhB homologs from *Yersinia pestis* biovar *microtus* expressed *in vivo* have differential Hfq-dependent stability. Res Microbiol 2012; 163:413-8; PMID:22659336; http://dx.doi.org/10.1016/j.resmic.2012.05.006
37. Zhang A, Wassarman KM, Rosenow C, Tjaden BC, Storz G, Gottesman S. Global analysis of small RNA and mRNA targets of Hfq. Mol Microbiol 2003; 50:1111-24; PMID:14622403; http://dx.doi.org/10.1046/j.1365-2958.2003.03734.x
38. van Kessel JC, Rutherford ST, Shao Y, Utria AF, Bassler BL. Individual and combined roles of the master regulators AphA and LuxR in control of the Vibrio harveyi quorum-sensing regulon. J Bacteriol 2013; 195:436-43; PMID:23204455; http://dx.doi.org/10.1128/JB.01998-12
39. Shao Y, Feng L, Rutherford ST, Papenfort K, Bassler BL. Functional determinants of the quorum-sensing non-coding RNAs and their roles in target regulation. EMBO J 2013; 32:2158-71; PMID:23838640; http://dx.doi.org/10.1038/emboj.2013.155
40. Overloper A, Kraus A, Gurski R, Wright PR, Georg J, Hess WR, Narberhaus F. Two separate modules of the conserved regulatory RNA AbcR1 address multiple target mRNAs in and outside of the translation initiation region. RNA Biol 2014; 11:624-40; PMID:24921646; http://dx.doi.org/10.4161/rna.29145
41. Durand S, Braun F, Lioliou E, Romilly C, Helfer AC, Kuhn L, Quittot N, Nicolas P, Romby P, Condon C. A nitric oxide regulated small RNA controls expression of genes involved in redox homeostasis in *Bacillus subtilis*. PLoS Genet 2015; 11:e1004957; PMID:25643072; http://dx.doi.org/10.1371/journal.pgen.1004957
42. Kuenne C, Billion A, Mraheil MA, Strittmatter A, Daniel R, Goesmann A, Barbuddhe S, Hain T, Chakraborty T. Reassessment of the *Listeria monocytogenes* pan-genome reveals dynamic integration hotspots and mobile genetic elements as major components of the accessory genome. BMC Genomics 2013; 14:47; PMID:23339658; http://dx.doi.org/10.1186/1471-2164-14-47
43. Bouloc P, Repoila F. Fresh layers of RNA-mediated regulation in Gram-positive bacteria. Curr Opin Microbiol 2016; 30:30-5; PMID:26773797; http://dx.doi.org/10.1016/j.mib.2015.12.008
44. Romby P, Charpentier E. An overview of RNAs with regulatory functions in gram-positive bacteria. Cell Mol Life Sci 2010; 67:217-37; PMID:19859665; http://dx.doi.org/10.1007/s00018-009-0162-8
45. Nielsen JS, Larsen MH, Lillebaek EM, Bergholz TM, Christiansen MH, Boor KJ, Wiedmann M, Kallipolitis BH. A small RNA controls expression of the chitinase ChiA in *Listeria monocytogenes*. PLoS One 2011; 6:e19019; PMID:21533114; http://dx.doi.org/10.1371/journal.pone.0019019
46. Nielsen JS, Lei LK, Ebersbach T, Olsen AS, Klitgaard JK, Valentin-Hansen P, Kallipolitis BH. Defining a role for Hfq in Gram-positive bacteria: evidence for Hfq-dependent antisense regulation in *Listeria monocytogenes*. Nucleic Acids Res 2010; 38:907-19; PMID:19942685; http://dx.doi.org/10.1093/nar/gkp1081
47. Zheng A, Panja S, Woodson SA. Arginine patch predicts the RNA annealing activity of Hfq from Gram negative and Gram positive bacteria. J Mol Biol 2016; PMID:27049793; http://dx.doi.org/10.1016/j.jmb.2016.03.027
48. Chang B, Halgamuge S, Tang SL. Analysis of SD sequences in completed microbial genomes: non-SD-led genes are as common as SD-led genes. Gene 2006; 373:90-9; PMID:16574344; http://dx.doi.org/10.1016/j.gene.2006.01.033
49. Caswell CC, Oglesby-Sherrouse AG, Murphy ER. Sibling rivalry: related bacterial small RNAs and their redundant and non-redundant roles. Front Cell Infect Microbiol 2014; 4:151; PMID:25389522; http://dx.doi.org/10.3389/fcimb.2014.00151
50. Shao Y, Bassler BL. Quorum-sensing non-coding small RNAs use unique pairing regions to differentially control mRNA targets. Mol Microbiol 2012; 83:599-611; PMID:22229925; http://dx.doi.org/10.1111/j.1365-2958.2011.07959.x
51. Michaux C, Verneuil N, Hartke A, Giard JC. Physiological roles of small RNA molecules. Microbiology 2014; 160:1007-19; PMID:24694375; http://dx.doi.org/10.1099/mic.0.076208-0
52. Hoe CH, Raabe CA, Rozhdestvensky TS, Tang TH. Bacterial sRNAs: regulation in stress. Int J Med Microbiol 2013; 303:217-29; PMID:23660175; http://dx.doi.org/10.1016/j.ijmm.2013.04.002
53. Vazquez-Boland JA, Kocks C, Dramsi S, Ohayon H, Geoffroy C, Mengaud J, Cossart P. Nucleotide sequence of the lecithinase operon of *Listeria monocytogenes* and possible role of lecithinase in cell-to-cell spread. Infect Immun 1992; 60:219-30; PMID:1309513
54. Gottschalk S, Bygebjerg-Hove I, Bonde M, Nielsen PK, Nguyen TH, Gravesen A, Kallipolitis BH. The two-component system CesRK

controls the transcriptional induction of cell envelope-related genes in *Listeria monocytogenes* in response to cell wall-acting antibiotics. J Bacteriol 2008; 190:4772-6; PMID:18456805; http://dx.doi.org/10.1128/JB.00015-08

55. Brondsted L, Kallipolitis BH, Ingmer H, Knochel S. kdpE and a putative RsbQ homologue contribute to growth of Listeria monocytogenes at high osmolarity and low temperature. FEMS Microbiol Lett 2003; 219:233-9; PMID:12620626; http://dx.doi.org/10.1016/S0378-1097(03)00052-1
56. Chakraborty T, Leimeister-Wachter M, Domann E, Hartl M, Goebel W, Nichterlein T, Notermans S. Coordinate regulation of virulence genes in *Listeria monocytogenes* requires the product of the *prfA* gene. J Bacteriol 1992; 174:568-74; PMID:1729245
57. Park SF, Stewart GS. High-efficiency transformation of Listeria monocytogenes by electroporation of penicillin-treated cells. Gene 1990; 94:129-32; PMID:2121618; http://dx.doi.org/10.1016/0378-1119(90)90479-B
58. Christiansen JK, Larsen MH, Ingmer H, Sogaard-Andersen L, Kallipolitis BH. The RNA-binding protein Hfq of *Listeria monocytogenes*: role in stress tolerance and virulence. J Bacteriol 2004; 186:3355-62; PMID:15150220; http://dx.doi.org/10.1128/JB.186.11.3355-3362.2004
59. Poyart C, Trieu-Cuot P. A broad-host-range mobilizable shuttle vector for the construction of transcriptional fusions to beta-galactosidase in gram-positive bacteria. FEMS Microbiol Lett 1997; 156:193-8; PMID:9513264; http://dx.doi.org/10.1016/S0378-1097(97)00423-0
60. Miller J. Experiments in Molecular Genetics. Cold Spring Harbor Laboratory Press 1972.
61. Zuker M. Mfold web server for nucleic acid folding and hybridization prediction. Nucleic Acids Res 2003; 31:3406-15; PMID:12824337; http://dx.doi.org/10.1093/nar/gkg595
62. Chevalier C, Geissmann T, Helfer AC, Romby P. Probing mRNA structure and sRNA-mRNA interactions in bacteria using enzymes and lead(II). Methods Mol Biol 2009; 540:215-32; PMID:19381563; http://dx.doi.org/10.1007/978-1-59745-558-9_16
63. Fechter P, Chevalier C, Yusupova G, Yusupov M, Romby P, Marzi S. Ribosomal initiation complexes probed by toeprinting and effect of trans-acting translational regulators in bacteria. Methods Mol Biol 2009; 540:247-63; PMID:19381565; http://dx.doi.org/10.1007/978-1-59745-558-9_18